ChemBioChem

Supporting Information

Flavin-Dependent Monooxygenases NotI and NotI′ Mediate Spiro-Oxindole Formation in Biosynthesis of the Notoamides**

Amy E. Fraley, Hong T. Tran, Samantha P. Kelly, Sean A. Newmister, Ashootosh Tripathi, Hikaru Kato, Sachiko Tsukamoto, Lei Du, Shengying Li, Robert M. Williams,* and David H. Sherman*

Author Contributions

A.F. Conceptualization:Equal; Data curation:Lead; Formal analysis:Lead; Investigation:Lead; Methodology:Lead; Validation:Lead; Writing - Original Draft:Lead; Writing - Review & Editing:Equal
H.T. Conceptualization:Supporting; Data curation:Supporting; Formal analysis:Supporting; Investigation:Equal; Methodology:Equal; Writing - Original Draft:Supporting
S.K. Data curation:Supporting; Formal analysis:Supporting; Investigation:Supporting
S.N. Data curation:Supporting; Formal analysis:Supporting; Investigation:Supporting
A.T. Data curation:Supporting; Investigation:Supporting; Supervision:Supporting; Validation:Supporting
H.K. Investigation:Lead; Resources:Supporting
S.T. Conceptualization:Supporting; Investigation:Supporting; Project administration:Supporting; Resources:Supporting; Supervision:Supporting; Writing - Review & Editing:Equal
L.D. Formal analysis:Supporting; Writing - Review & Editing:Equal
S.L. Conceptualization:Equal; Formal analysis:Supporting; Investigation:Supporting; Project administration:Supporting; Supervision:Supporting; Writing - Review & Editing:Equal
R.W. Conceptualization:Equal; Funding acquisition:Equal; Investigation:Equal; Project administration:Supporting; Resources:Equal; Supervision:Supporting; Writing - Original Draft:Supporting; Writing - Review & Editing:Equal
D.S. Conceptualization:Equal; Funding acquisition:Equal; Investigation:Equal; Project administration:Equal; Resources:Equal; Supervision:Equal; Writing - Original Draft:Equal; Writing - Review & Editing:Equal

Experimental Methods:

1. Fungal strains and culture conditions

Aspergillus amoenus and *Aspergillus protuberus* spores were generated on YPD agar plates over the course of seven days. Each plate of spores was harvested into 5 mL sterile water by gently scraping the surface of the culture with a sterile inoculating loop. Spores were stored at -80°C prior to genomic DNA extraction. Genomic DNA was harvested using Wizard Genomic DNA Purification Kit from Promega.

2. cDNA preparation and cloning of *notI* and *notI′*

Total RNA was extracted from the mycelia of *Aspergillus protuberus* using the Invitrogen PureLink RNA Mini Kit and corresponding plant tissue processing protocol. The culture was grown statically on liquid medium (50% seawater with 2.0% malt extract and 0.5% peptone) at 28°C and dried by filtration on the 17th day (roughly 500 mg fungal mat). RNA was treated with DNase I, and cDNA was generated using Invitrogen Superscript First Strand Synthesis. PCR was used to amplify *notI* from the cDNA template. Additionally, a codon optimized construct was purchased from GeneArt, Life Technologies and used in all enzymology studies. The codon optimized *notI* was inserted into the *pMCSG7* vector by ligation independent cloning (LIC). To generate *notI′*, introns were predicted by analysis using Softberry Fgenesh-M. Further analysis was performed by comparison with the *notI* sequence, which has 81% DNA sequence identity. The *notI′* gene was amplified from genomic DNA using overlapping PCR with primers in Table S1. The amplified gene was cloned into a pET28b vector with an MBP tag using restriction enzyme digest and ligation. Plasmids were transformed into *E. coli* DH5α for screening and plasmid maintenance.

3. Overexpression and purification of protein for enzymology

The *Escherichia coli* BL21 (DE3) transformant containing *pMCSG7-notI* and Takara chaperone plasmid *pGKJE8* was grown at 37°C overnight in LB media containing 50 μg/mL of ampicillin and 25 μg/mL of chloramphenicol. 25 mL of culture were used to inoculate 1 L of TB media containing the aforementioned concentrations of antibiotic and 4% glycerol, and cultures were supplemented with 0.5 mg/mL L-arabinose and 5 ng/mL tetracycline to induce chaperone expression. Cells were grown at 37°C for roughly 4 hours until A_{600} reached 0.6-1.0, and isopropyl β-D-thiogalactoside (IPTG, 0.2 mM) and riboflavin (50 μM) were added to induce protein overexpression overnight at 18°C. The *Escherichia coli* BL21 *pRARE* transformant containing *pET28b-MBP-notI′* and Takara chaperone plasmid *pTf16* was grown at 37°C overnight in LB media containing 50 μg/mL of kanamycin, 25 μg/mL of chloramphenicol, and 100 μg/mL of spectinomycin. 5 mL of culture was used to inoculate 1 L of TB media containing the aforementioned concentrations of antibiotic and 4% glycerol, and cultures were supplemented with 0.5 mg/mL L-arabinose to induce chaperone expression. Cells were grown at 37°C for roughly 4 hours until A_{600} reached 0.6-1.0, and isopropyl β-D-thiogalactoside (IPTG, 0.2 mM) and riboflavin (50 μM) were added to induce protein overexpression overnight at 18°C.

All purification steps were conducted at 4°C. Briefly, 1 L of expression culture was spun down at 5,500 rpm. The harvested cell pellet was resuspended in 35 ml of lysis buffer (10 mM imidazole pH 8, 50 mM NaH_2PO_4, 300 mM NaCl, 10% v/v glycerol, adjusted to pH 8) with the addition of 10 mg lysozyme, 4 mg DNase, 50 μM flavin adenine dinucleotide (FAD), 2 mM $MgSO_4$ and lysed by sonication. Insoluble material was removed by centrifugation at 20,000 rpm for 30 minutes, and the supernatant was filtered. NotI and NotI′ were purified through metal affinity chromatography with Ni^{2+}-NTA resin (Novagen) that was equilibrated with lysis buffer. The protein-bound resin was washed with 50 mL of lysis buffer, 50 mL of wash buffer (20 mM imidazole pH 8, 50 mM NaH_2PO_4, 300 mM NaCl, 10% v/v glycerol, adjusted to pH 8), and finally 10 mL of elution buffer (250 mM imidazole pH 8, 50 mM NaH_2PO_4, 300 mM NaCl, 10% v/v glycerol, adjusted to pH 8). Protein in the eluate was exchanged into storage buffer (50 mM NaH_2PO_4, 1 mM EDTA, 0.2 mM DTT, 10% v/v glycerol, pH 7.3) using a PD-10 column. Samples were then flash frozen with liquid N_2 and stored at -80°C. A 1L expression culture yielded ~ 42 mg of NotI and ~ 15 mg of NotI′.

4. Enzymatic assays and Q-TOF LC-MS analysis of NotI and NotI′ reactions with deoxybrevianamide E (13), 6-OH-deoxybrevianamide E (14), notoamide S (15), notoamide E (1), (+)/(-)- notoamide T (16/17).
The standard enzyme assay containing 0.5 mM substrate, 2.5 mM NADH, and 20 μM enzyme in 100 μL reaction buffer (50 mM NaH_2PO_4, 1 mM EDTA, 0.2 mM DTT, 10% v/v glycerol, pH 7.3) was performed at 28°C overnight. Each reaction was extracted three times with 200 μL chloroform, and the extract was dried down under N_2 gas. The product was resuspended in 100 μL methanol for Q-TOF LC-MS analysis. The samples were analyzed by QTOF LC-MS using a ZORBAX Eclipse Plus C18 reverse phase column (3.5 μm, 4.6 x 150 mm), monitoring wavelengths 240 nm and 280 nm and scanning 200 to 1200 m/z with the following time program: solvent A: water + 0.1% formic acid and solvent B: 95% acetonitrile in water + 0.1% formic acid; flow rate: 20% B over 2 minutes, 20-100% B over 10 minutes, 100% B over 5 minutes, 100-20% B over 1 minutes, 20% B over 5 minutes. The flow rate was 0.8 mL/min. The large-scale reaction to produce notoamide TI (**18**) was performed under the same reaction conditions with 0.5mM racemic notoamide T (**16**/**17**) on a 10 mL scale to produce 2 mg of final product. The reaction was extracted with chloroform, as described above, and purified by reversed phase HPLC.

5. Enzymatic assays and HPLC analysis of NotI and NotI′ reactions with (+)-stephacidin A (9), (-)-stephacidin A (4), (+)-6-*epi*-stephacidin A (6), and (-)-6-*epi*-stephacidin A (*7*).
The standard enzyme assay containing 200 μM FAD, 50 μM substrate, 5 mM NADH, and 40 μM enzyme in 50 μL reaction buffer (50 mM NaH_2PO_4, 1 mM EDTA, 0.2 mM DTT, 10% v/v glycerol, pH 7.3) was performed at 28°C for 2 hours. The reactions were quenched and extracted three times by the addition of 100 μL ethyl acetate. The ethyl acetate was removed by evaporation under N_2, and the purified reaction mixture was resuspended in 50 μL LC-MS grade methanol. The samples were compared to product standards on a Shimadzu HPLC using a Phenomenex Lux 5 μm Cellulose-3 LC column (250 x 4.6 mm) with the following time program: 30% acetonitrile for 2 minutes, 30-60% acetonitrile over 15 minutes, 60% acetonitrile for 1 minute, 60-30% acetonitrile over 1 minute, and 30% acetonitrile for 8 minutes. The flow rate was 1 mL/min and the reactions were monitored at 240nm.

6. NotI kinetic assays and Q-TOF LC-MS analysis
The reactions were performed with varying substrate concentrations (10-500 μM (-)-stephacidin A (**4**)) on a 250 μL scale containing 2.5 μM NotI, 5 mM NADH, and 0.1 mM FAD in reaction buffer (50 mM NaH_2PO_4, 1 mM EDTA, 0.2 mM DTT, 10% v/v glycerol, pH 7.3). The reactions were pre-warmed at room temperature for 5 minutes and initiated with addition of 5 mM NADH. At varying time points, the reactions were quenched with an equal volume methanol, vortexed vigorously, and placed on ice. The samples were then centrifuged at 17,000 xg at 4°C for 25 minutes to pellet the precipitated protein, and the supernatant was used for Q-TOF LC-MS analysis. The samples were analyzed using a ZORBAX Eclipse Plus C18 reverse phase column (3.5 μm, 4.6 x 150 mm), monitoring at 240 nm/280 nm and scanning 200 to 1200 m/z using the following time program: solvent A: water + 0.1% formic acid, solvent B: 95% acetonitrile in water + 0.1% formic acid; flow rate: 0.8 mL/min; mobile phase: 50% B over 2 minutes, 50-55% B over 5 minutes, 55-50% B over 30 seconds, 50% B over 2.5 minutes. All experiments were performed in duplicate. Quantitative analysis was performed through integration of the extracted ion chromatograms corresponding to substrate and product masses. The data were fit to the Michaelis-Menten model.

7. NotI epodixation efficiency reactions
To measure the rate of NADH oxidation during the NotI/NotI′-catalyzed conversion of (-)-stephacidin A (**4**), 50 μL reactions were run in a 384-well plate and monitored at 340 nm at various timepoints over 45 minutes. The reaction components consisted of 2.5 μM FAD, 2.5 μM NotI, 200 μM (-)-stephacidin A (**4**), and 200 μM NADH. Separate aliquots were quenched at 10, 20, 30, and 40 minutes and analyzed by the above described HPLC method to determine product formation under identical conditions to the NADH assays.

8. Determination of FAD incorporation in NotI and NotI′

Each protein was denatured by boiling and centrifugation and the cofactor identification was monitored by HPLC with a Phenomenex LUNA phenyl-hexyl 100A LC column (250 x 4.6 mm). The samples were monitored at 448nm using the following method for separation: 5%B for 2 minutes, 5-30%B over 10 minutes, hold 30%B for 2 minutes, 30-100%B over 1 minute, hold 100%B for 2 minutes, 100-5%B over 2 minutes, where solvent A = water + 0.1% formic acid and B = acetonitrile + 0.1% formic acid with a flow rate of 1mL/min. FAD incorporation was determined through the use of a standard curve for FAD, from which the concentration of the cofactor was determined and compared to the concentration of the enzyme.

Table S1. Primers for *notI* and *notI′* intron removal and amplification

Name	**Sequence**	**Function**
*notI*_F	GGAGTTCCATATGGCTATAGACGGATCT	amplification
*notI*_F	CAATGAAGCTTTCAACCAACCGGTATACC	amplification
*notI′*_F_NdeI	GGAATTCCATATGGCTATAGACGCATCTGGTGCTG	amplification
*notI′*_R	ATAAGAATGCGGCCGCTTAATCCACCGGTATACCACCGAAG	amplification
notI′_MBP_F	CTAGTGAGAATCTCTACTTCCAAGGCGCTATGGCTATAGACGCATCTGGTGC	amplification
notI′_MBP_R	GGTGGTGCTCGAGTGCGGCCGCAAGTTAATCCACCGGTATACCACCG	amplification
*notI′*_Int1_F	CAAGAGCTACCGTTTGGG AGACTTGATCAATGTGACCGGG	intron removal
*notI′*_Int1_R	CCCGGTCACATTGATCAAGTCTCCCAAACGGTAGCTCTTG	intron removal
*notI′*_Int2_F	CGAGTGACAGAGAAGCTAAGGTACCAAAGGGTTGCTGCAA	intron removal
*notI′*_Int2_R	TTGCAGCAACCCTTTGGTACCTTAGCTTCTCTGTCACTCG	intron removal

Table S2. ^{13}C-NMR, ^{1}H-NMR, gHMBCAD, and gCOSY correlations recorded at 700 MHz in $(CD_3)_2SO$-d_6 for notoamide TI (**18**) isolated from *in vitro* reaction with NotI. HRMS (ESI-QTOF): m/z $[M+H]^+$ calculated for $C_{26}H_{31}N_3O_4$ = 450.2393, experimental = 450.2414. Data were measured on a Varian Vnmrs 700 spectrometer.

Position	∂ ^{13}C	∂ ^{1}H (m, *J* [Hz])	gHMBCAD	gCOSY
1	43.37	3.38 obs		
2	29.03	1.78 (m)		
		2.50 obs	1,3,4,21	3
3	24.34	1.78 (m)	5	2
		1.99 (m)		
4	68.08			
5	29.57	1.72 (dd, 12.8, 8.3)	4,6,7,21	
		1.92 (m)		6
6	55.39	3.24 (m)	7,18	
7	44.92			
8	61.36			
9	120.29			
10	107.49	6.41 (d, 8.0)	9,14	11
11	123.64	6.81 (d, 8.0)	12,13	10
12	141.35			
13	155.27			
14	110.05			
15	NH	8.51		
16	183.39			
17	33.34	2.14 (d, 14.1)	7,8,16,18,19	
		2.78 (d, 14.2)	6,8,9,16,18,19	
18	65.53			
19	169.48			
20				
21	173.13			
22	NH	9.07	4	
23	23.46	3.17 (m)	12,13,14,24,25	24
24	122.66	5.13 (t, 7.0)		25
25	130.43			
26	25.57	1.61 (d, 10.1)	24,25,27	
27	17.83	1.69 (s)	24,25,26	
28	23.09	0.68 (s)	6,7,8,29	
29	19.56	0.70 (s)	28	

*obs: These peaks are obscured by the solvent and water in the sample.

Table S3. Percent identity matrix of NotI/NotI′ homologs including AuaG,[1] PhqK,[2] OxaD,[3] asperlicin C monooxygenase (GenBank: GBF62818.1), FMO from *Penicillium griseofulvum* (GenBank: KXG49074.1), NotI, NotI′, NotB,[4], and BvnB[5] (generated using Clustal2.1).[6]

	AuaG	PhqK	OxaD	Asperlicin C FMO	*P. griseofulvum*	NotI	NotI'	NotB	BvnB
AuaG	100.00	25.33	25.86	22.75	20.37	25.20	26.26	23.48	24.40
PhqK	25.33	100.00	33.71	35.78	33.55	34.91	33.96	31.82	32.34
OxaD	25.86	33.71	100.00	35.43	41.14	36.72	37.88	36.20	35.57
Asperlicin C FMO	22.75	35.78	35.43	100.00	44.30	42.13	41.44	38.48	35.51
P. griseofulvum	20.37	33.55	41.14	44.30	100.00	40.51	39.81	44.15	42.95
NotI	25.20	34.91	36.72	42.13	40.51	100.00	84.99	45.03	42.92
NotI'	26.26	33.96	37.88	41.44	39.l81	84.99	100.00	43.42	41.76
NotB	23.48	31.82	36.20	38.48	44.15	45.03	43.42	100.00	62.14
BvnB	24.40	32.34	35.57	35.51	42.95	42.92	41.76	62.14	100.00

Table S4. Average percent conversions for NotI and NotI′ with natural substrates (+)-stephacidin A (**9**), (-)-stephacidin A (**4**), (+)-6-*epi*-stephacidin A (**6**), and (-)-6-*epi*-stephacidin A (**7**). Reactions were performed in triplicate and conversions were calculated via substrate and product standard curves.

Substrate	Product	NotI conv (%)	NotI′ conv (%)
(+)-Stephacidin A (**9**)	(-)-Notoamide B (**10**)	11	9
(-)-Stephacidin A (**4**)	(+)-Notoamide B (**5**)	68	52
(+)-6-*epi*-Stephacidin A (**6**)	(+)-Versicolamide B (**8**)	13	7
(-)-6-*epi*-Stephacidin A (**7**)	(-)-Versicolamide B (**11**)	0	0

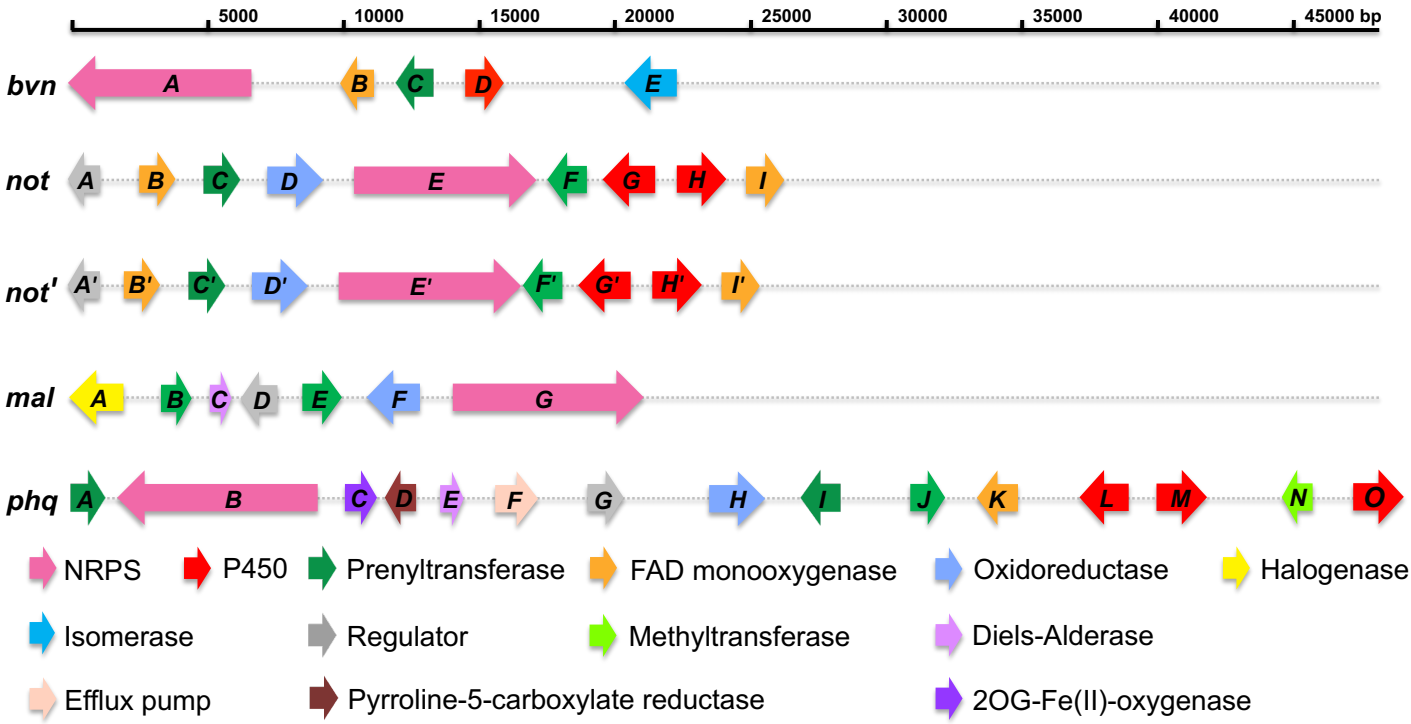

Figure S1. Comparative biosynthetic gene clusters for bicyclo[2.2.2]diazaoctane fungal indole alkaloids, including brevianamide (*bvn*), notoamide (*not/not'*), malbrancheamide (*mal*), and paraherquamide (*phq*).

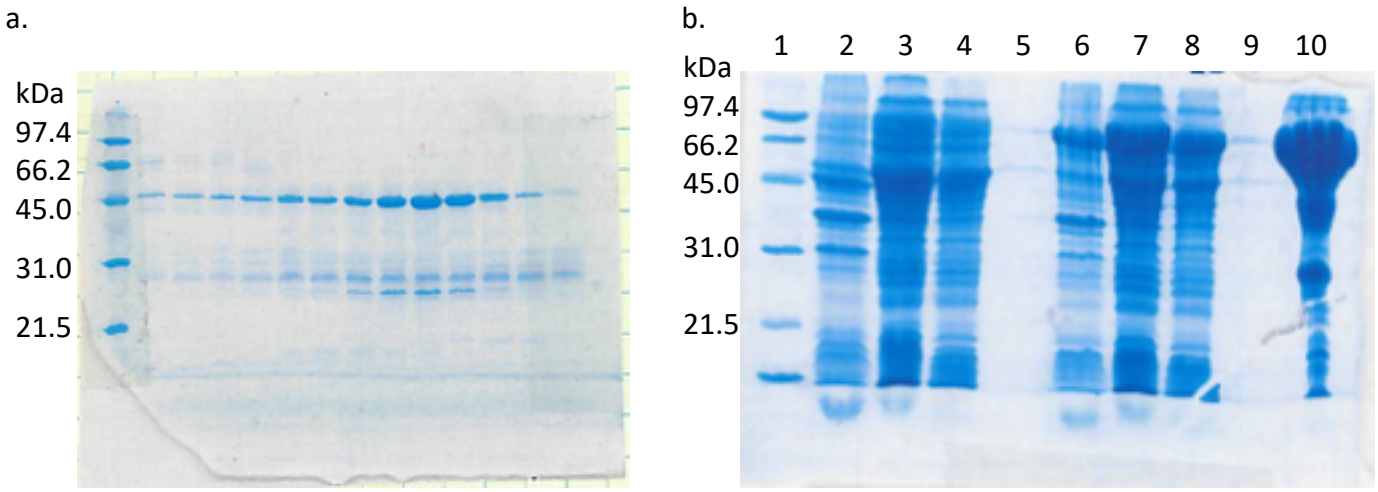

Figure S2. SDS-PAGE gels from purification of a.) NotI (47,044 Da) and b.) MBP-NotI′ (89,544 Da). NotI was purified via a gradient elution with increasing concentrations of imidazole to yield ~ 42 mg of protein per liter of expression culture. NotI′ was fused to an N-terminal MBP tag and batch purified resulting in 15 mg of protein per liter of expression culture. Columns 2-5 represent an attempt to express NotI′ in the pTrc vector, while the MBP-fusion resulted in majority soluble protein (columns 7 supernatent and 10 elution with 250 mM imidazole) and some insoluble protein (column 6 cell debri pellet and 8 flowthrough from the Ni column).

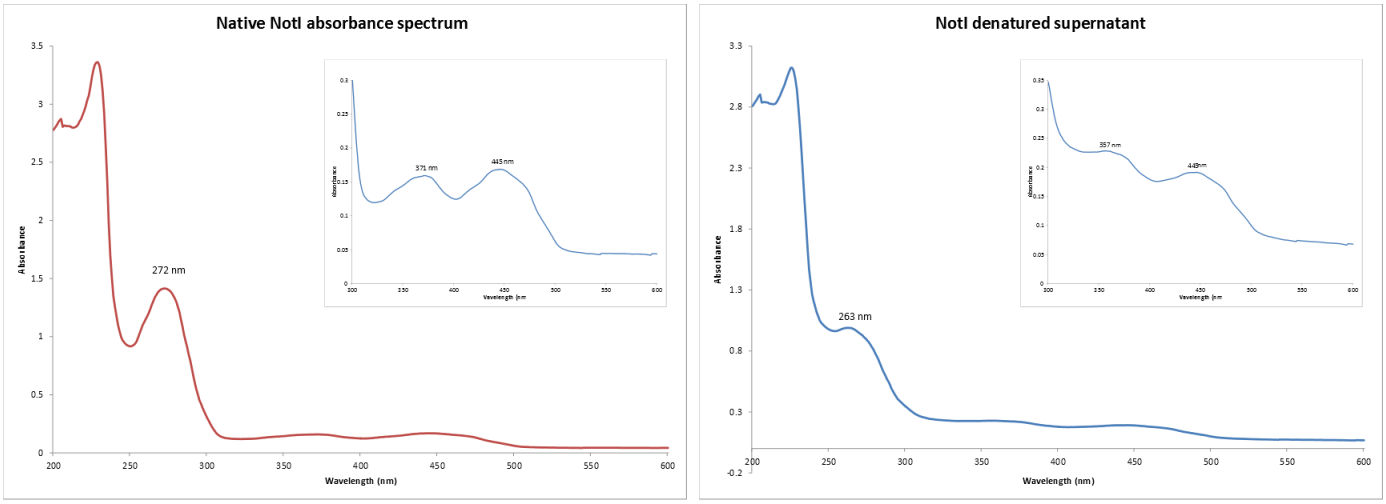

Figure S3. UV-Vis spectra of purified NotI protein solution (left) and the supernatant of denatured NotI protein solution (right). Denatured protein was generated by boiling for 15 minutes. The flavin cofactor peaks at 360 and 450 nm are present in both the native protein solution and the denatured supernatant.

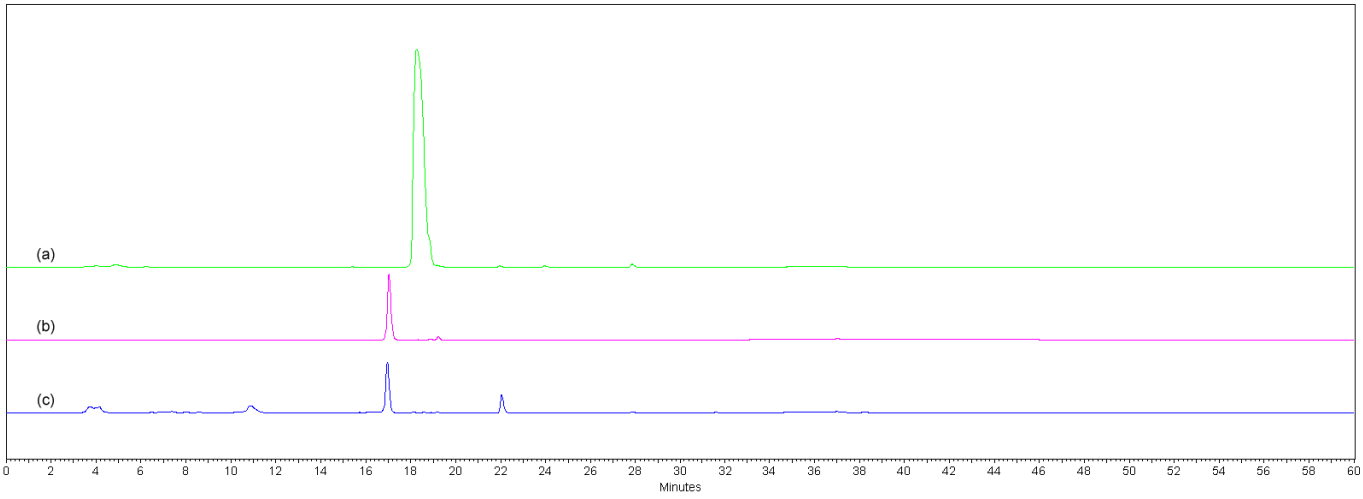

Figure S4. Identification of FAD as the non-covalently bound NotI flavin cofactor. (a) FMN standard; (b) FAD standard; (c) NotI supernatant after denaturation of protein by boiling and centrifugation.

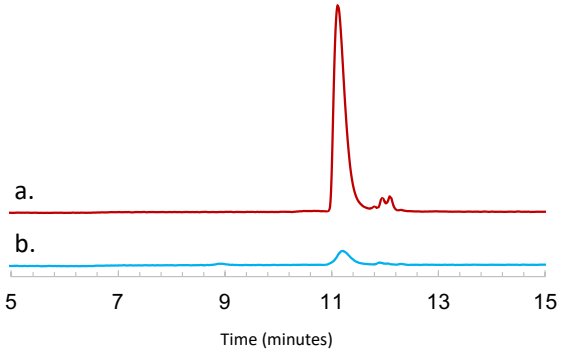

Figure S5. Identification of FAD as the non-covalently bound NotI′ flavin cofactor by HPLC monitored at 448nm. (a) FAD standard; (b) NotI′ supernatant after denaturation of protein by boiling and centrifugation.

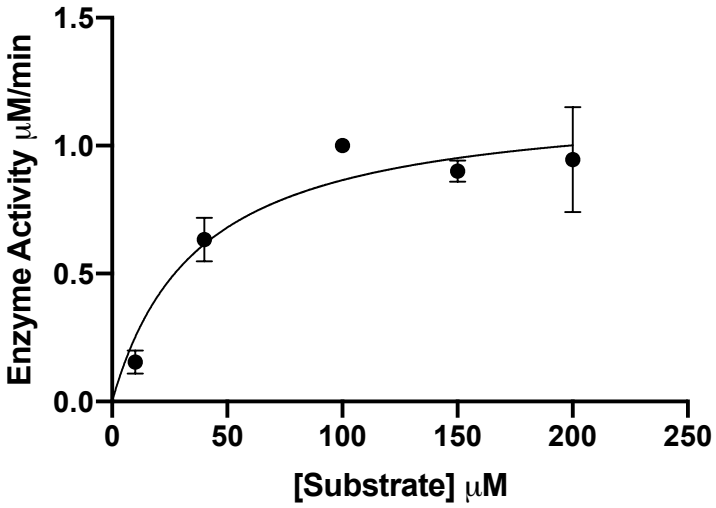

Figure S6. Kinetic curve of NotI against (-)-stephacidin A (**4**).

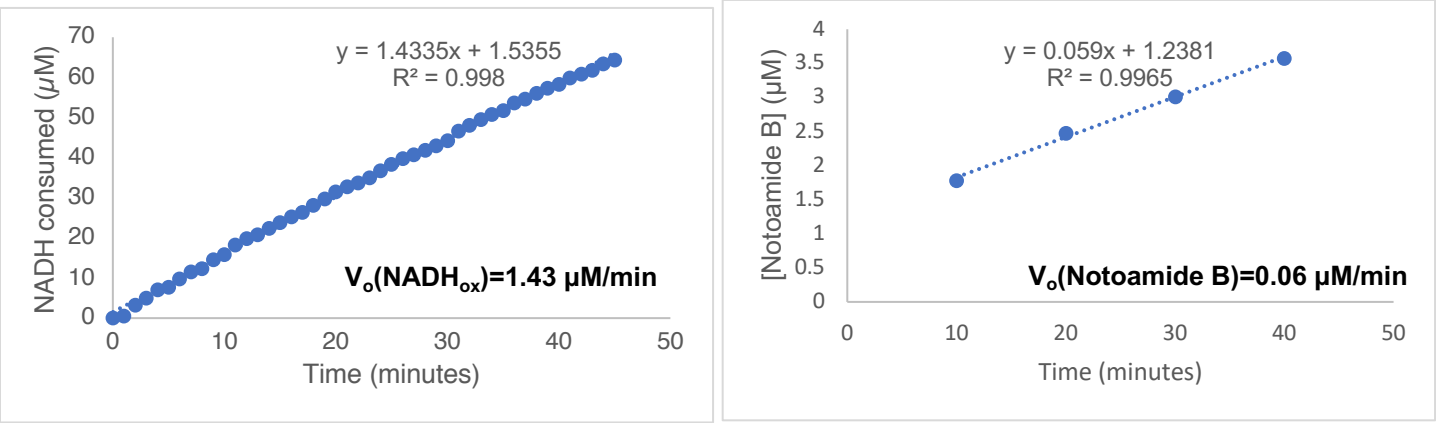

Figure S7. Comparison of the rate of NADH oxidation and the average rate of product formation in a reaction with NotI and (-)-stephacidin A (**4**). The higher rate of NADH oxidation indicates decoupling of these two catalytic factors, and the epoxidation efficiency is 4.1%.

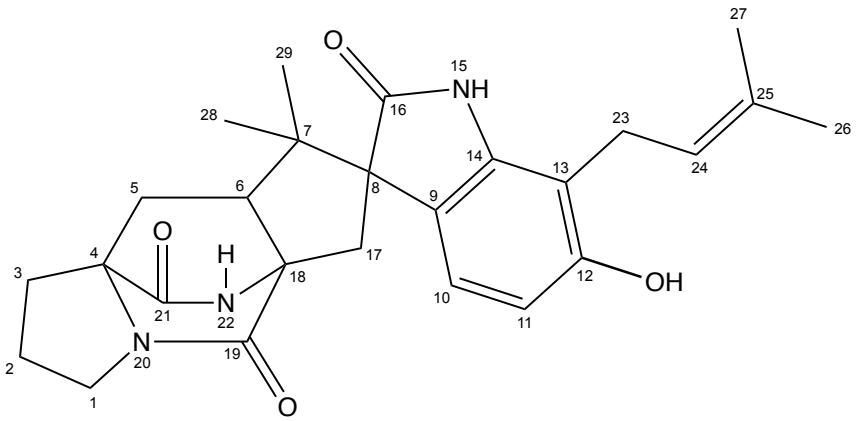

Figure S8. Numbering scheme for notoamide TI (**18**).

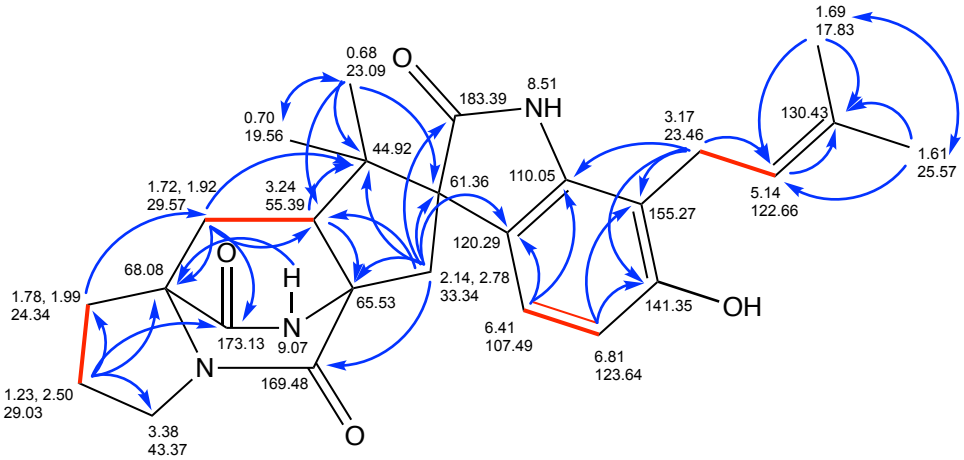

Figure S9. Planar structure of Notoamide TI (**18**) showing gCOSY correlations with bold red bonds and gHMBCAD correlations with blue arrows recorded at 700 MHz in $(CD_3)_2SO$-d_6.

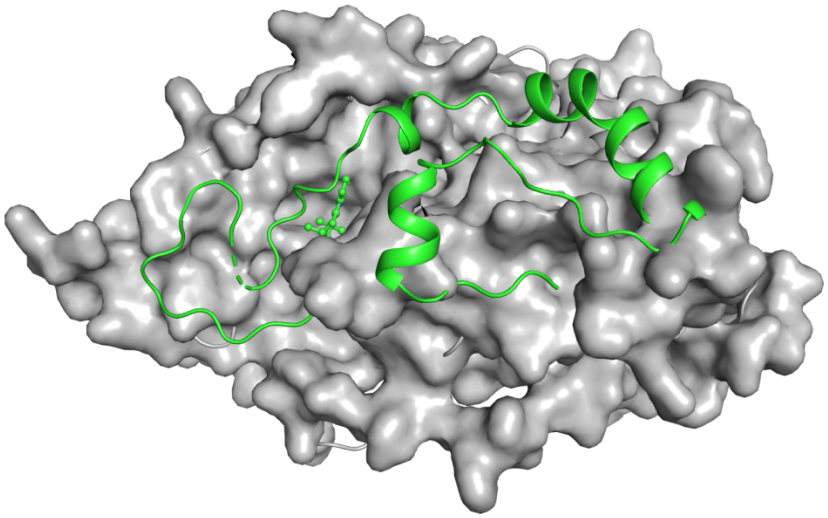

Figure S10. C-terminus and substrate paraherquamide L from PhqK crystal structure (green, PDB ID: 6pvi) aligned with the surface representation of the NotI homology model.

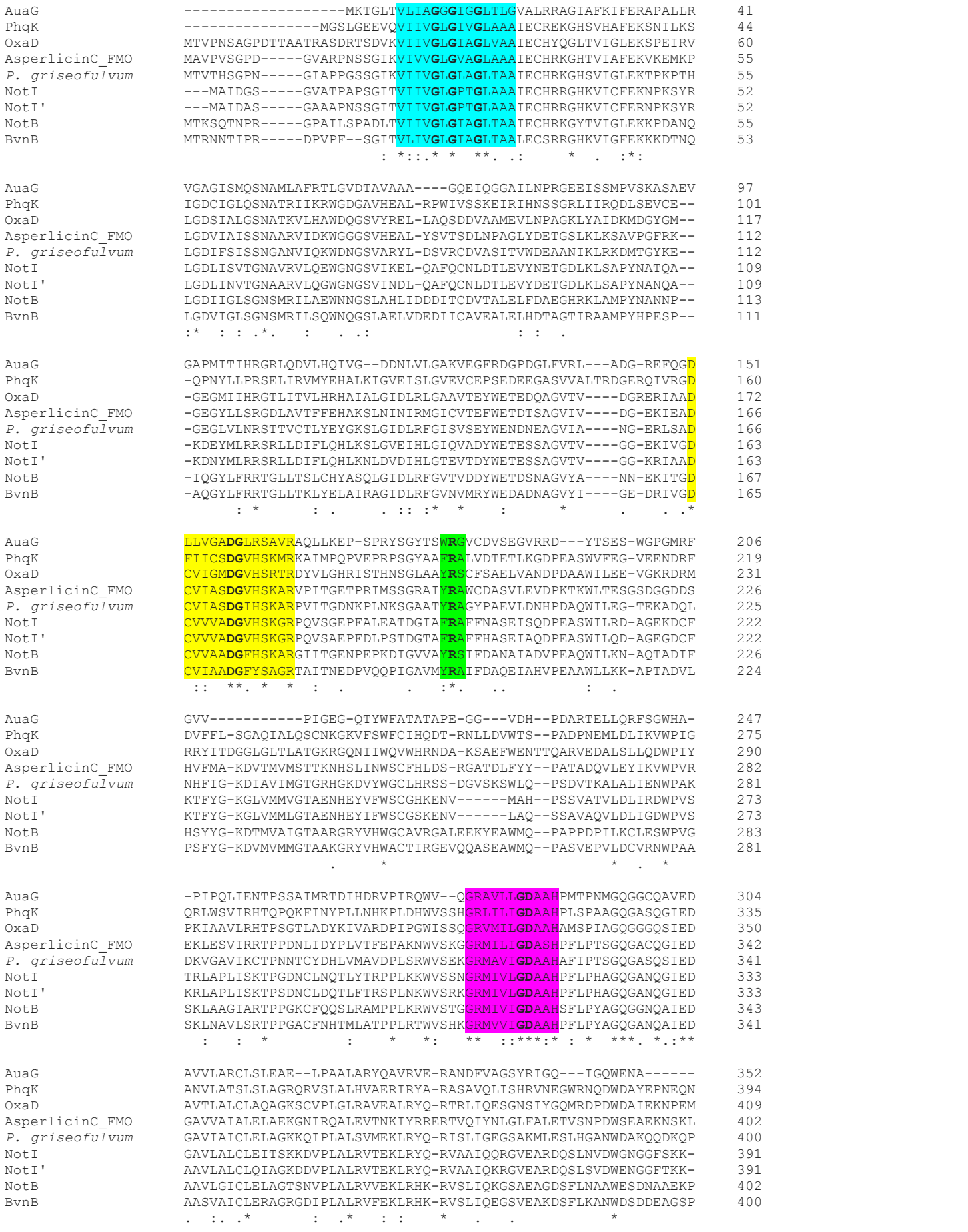
AuaG
PhqK
OxaD
AsperlicinC_FMO
P. griseofulvum
NotI
NotI'
NotB
BvnB

```
AuaG                -----FACWVREKLMRMMSSDRVD---ARTRRNLQFTPL----------------------     383
PhqK                IASLPLETWIYGHDSQAYTEQEFEMVVRAVQEGEEYHATNLPDKLRVQLG--IRNVDVKE     452
OxaD                I-KFPRPQWIFGYDARRDVSEEFPTVKKAIEEGSEYRPRNIPEDCQYQIVHDYKKTVST-     467
AsperlicinC_FMO     F-AIPNPEWVLNHNCQKSAYDEYHKIAESIANGTEYTPQNIPSSAVRS------------     449
P. griseofulvum     T-LIARAMWIFDHDCQKSTYEEFEKAAEAVVSGSTYVPANIPNDGRHGIVEEEGKSTVKV     459
NotI                --LTLHPAWLHDHDCIKQVYEEFDKAADAVTKGHEHTFGGIPVG----------------     433
NotI'               --LTLYPAWLHDQDCIKQVYEEFDKAVAAVTKGHECTFGGIPVD----------------     433
NotB                T-AFTHQAWVYAHNCVDHAYEQFNAAAEAVMNGWEYTPTNIPANGKFRQEEG--NI----     455
BvnB                S-AYLHQSWVYNHDCVQHVVEEFQTAADAIRHGRKYIPTNVPVDGKYRQE----------     449
                           *:          :.          .

AuaG                -----------      383
PhqK                PLQNKSP----      459
OxaD                -----------      467
AsperlicinC_FMO     -----------      449
P. griseofulvum     PSAHSAPISAE      470
NotI                -----------      433
NotI'               -----------      433
NotB                -----------      455
BvnB                -----------      449
```

Figure S11. Sequence alignment of flavin-dependent monooxygenases (FMOs) including AuaG,[1] PhqK,[2] OxaD,[3] asperlicin C monooxygenase (GenBank: GBF62818.1), FMO from *Penicillium griseofulvum* (GenBank: KXG49074.1), NotI, NotI′, NotB,[4], and BvnB[5] performed using Clustal2.1.[6] The proposed catalytic arginine is highlighted in bold in the green section. The first FAD-binding motif or the Rossmann fold (*βαβ*-fold, containing GxGxxG) is shown highlighted in cyan, the second FAD-binding motif (GD sequence) is shown highlighted in magenta, and the DG motif is highlighted in yellow.[7]

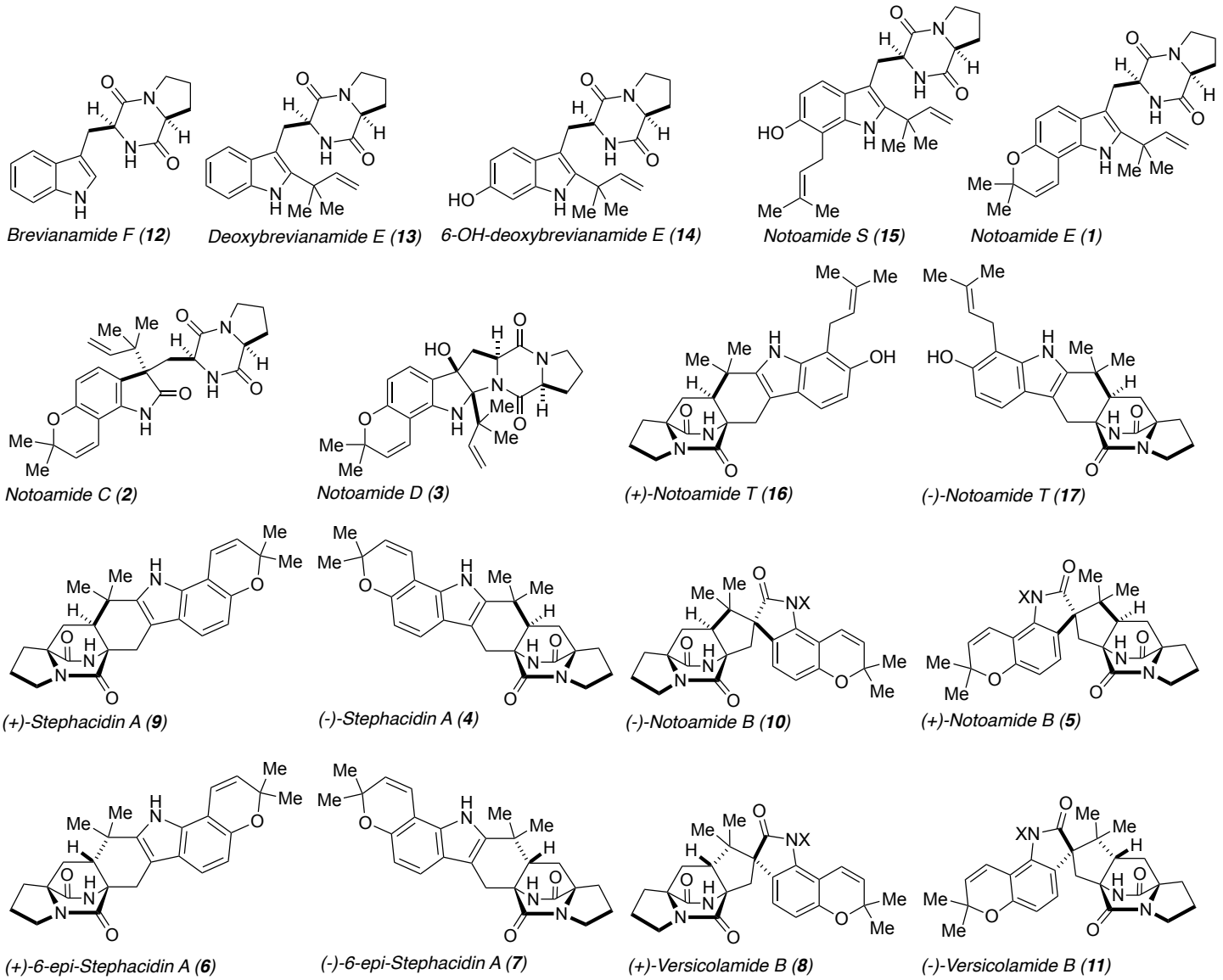

Figure S12. Substrates and products from reactions with NotI and NotI′. (-)-versicolamide B (**11**) has not been isolated from *Aspergillus amoenus* or *Aspergillus protuberus*.

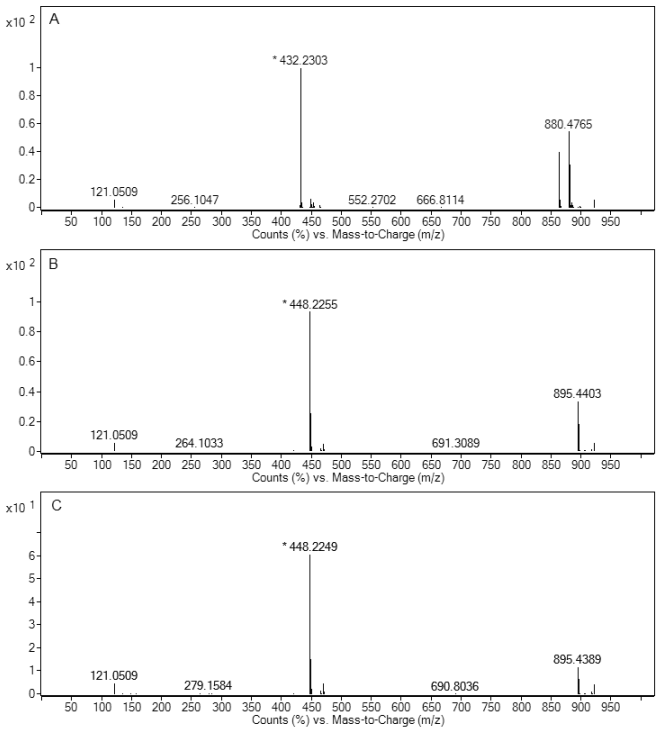

Figure S13. Mass spectra (MS) of (A) (-)-stephacidin A (**4**), expected $[M+H]^+$ = 432.2287; (B) (+)-notoamide B (**5**) formed from reaction with NotI, expected $[M+H]^+$ = 448.2236; (C) (+)-notoamide B (**5**) formed from reaction with NotI′), expected $[M+H]^+$ = 448.2236. Data were measured on an Agilent Q-TOF LC-MS.

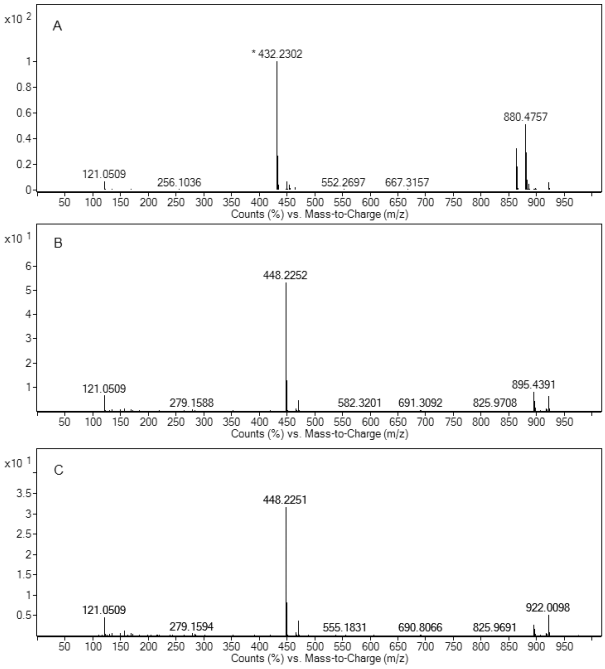

Figure S14. Mass spectra of (A) (+)-stephacidin A (**9**) standard expected $[M+H]^+$ = 432.2287; (B) (-)-notoamide B (**10**) produced by NotI, expected $[M+H]^+$ = 448.2236; (C) (-)-notoamide B (**10**) produced by NotI′ expected $[M+H]^+$ = 448.2236. Data were measured on an Agilent Q-TOF LC-MS.

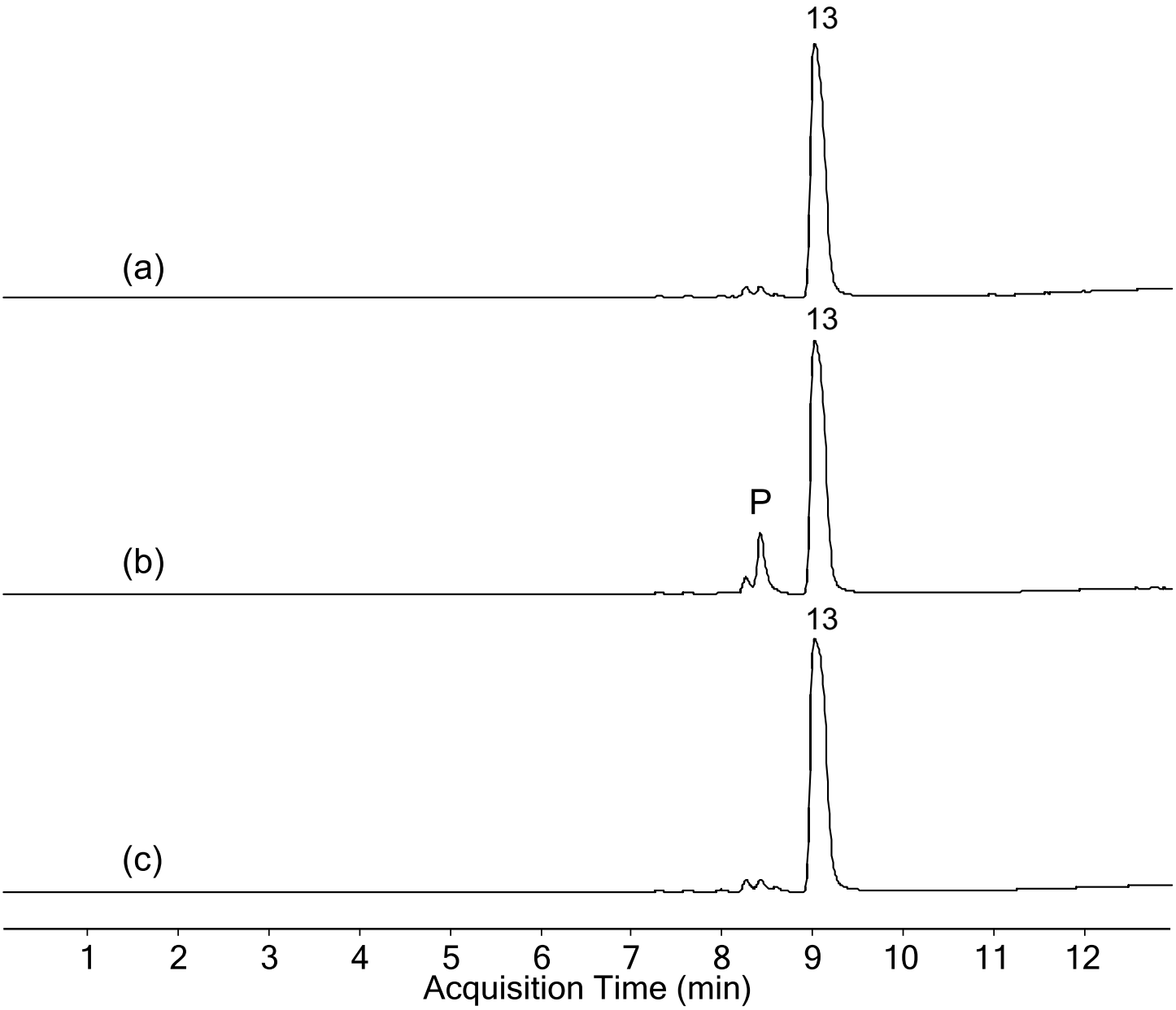

Figure S15. Q-TOF LC-MS analysis depicting EICs of (a) NotI′ reaction with deoxybrevianamide E (**13**); (b) NotI reaction with **13**; (c) no enzyme control with **13**. Product formed is denoted with **P**. Data were measured on an Agilent Q-TOF LC-MS.

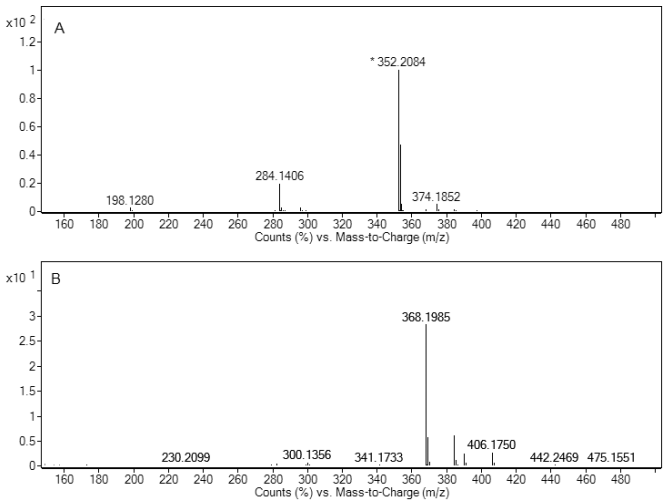

Figure S16. Mass spectra of (A) deoxybrevianamide E (**13**) standard, expected $[M+H]^+$ = 352.2025; (B) Product formed from NotI reaction with **13**, expected $[M+H]^+$ = 368.1974. Data were measured on an Agilent Q-TOF LC-MS.

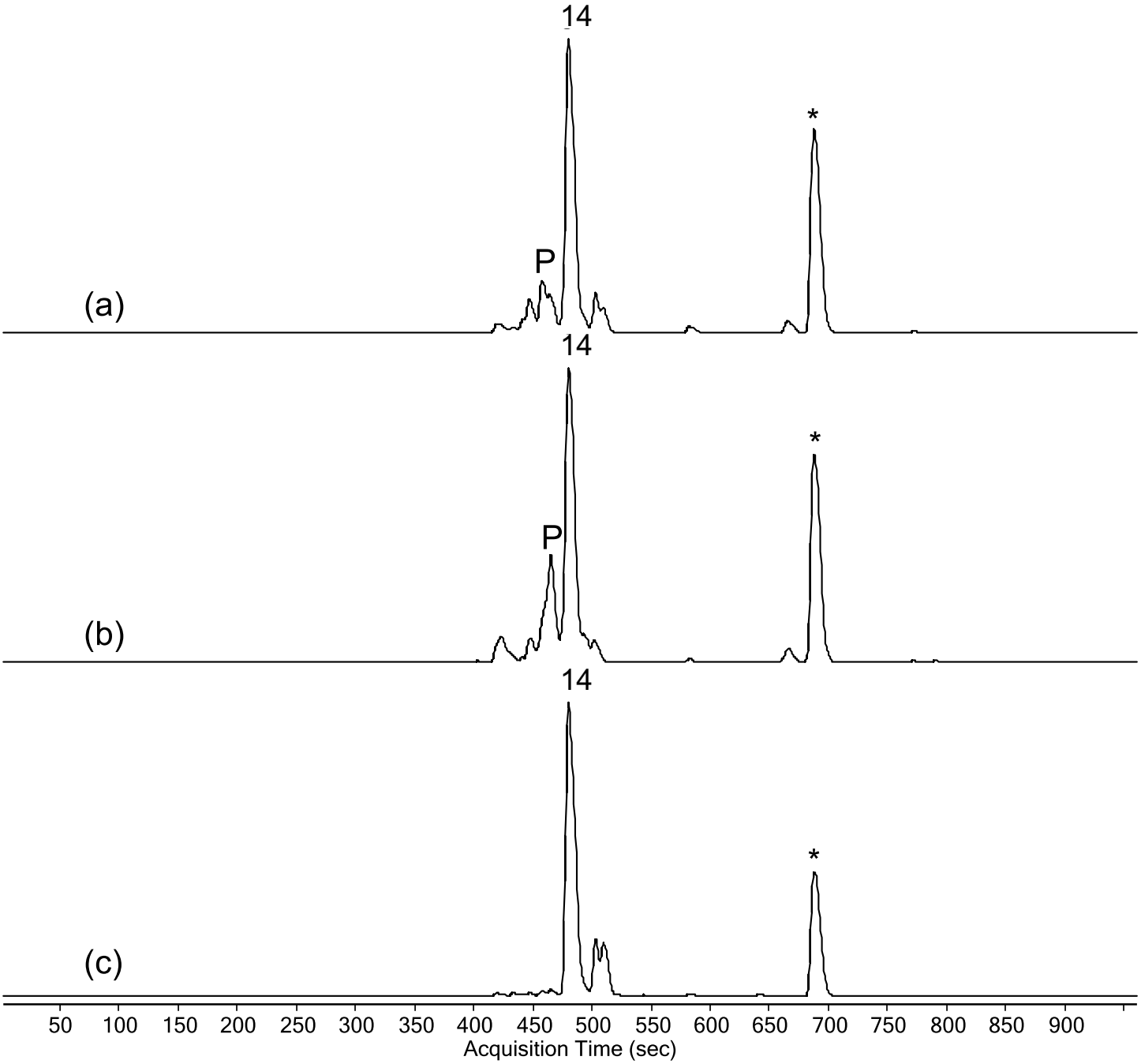

Figure S17. Q-TOF LC-MS analysis depicting EICs of (a) NotI′ reaction with 6-OH-deoxybrevianamide E (**14**); (b) NotI reaction with **14**; (c) no enzyme control with **14**. Products formed are denoted with **P**. Asterisk denotes a possible diastereomer of **14**. Data were measured on an Agilent Q-TOF LC-MS.

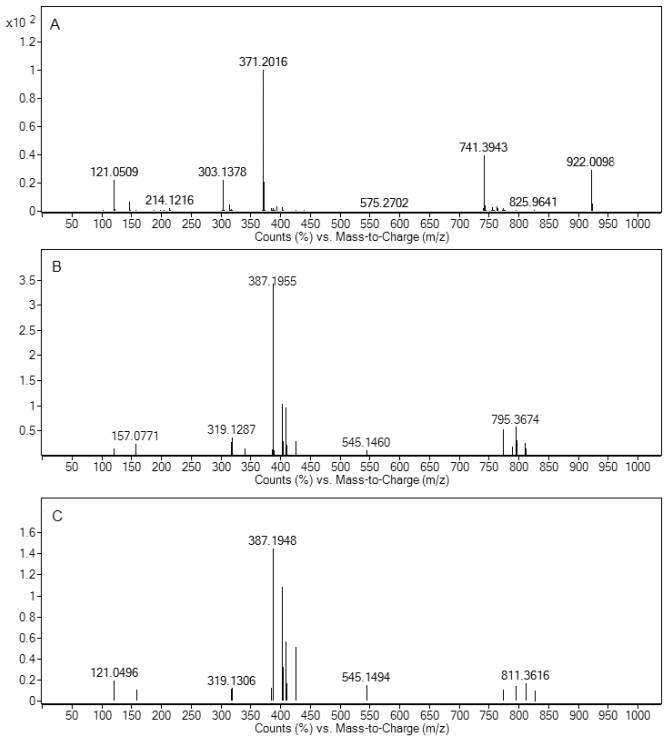

Figure S18. Mass spectra of (A) 6-OH-deoxybrevianamide E (**14**) standard labelled with three ^{13}C atoms, expected $[M+H]^+$ = 371.1974; (B) Product formed from NotI reaction with **14**, expected $[M+H]^+$ = 387.1923; (C) Product formed from NotI′ reaction with **14**, expected $[M+H]^+$ = 387.1923. Data were measured on an Agilent Q-TOF LC-MS.

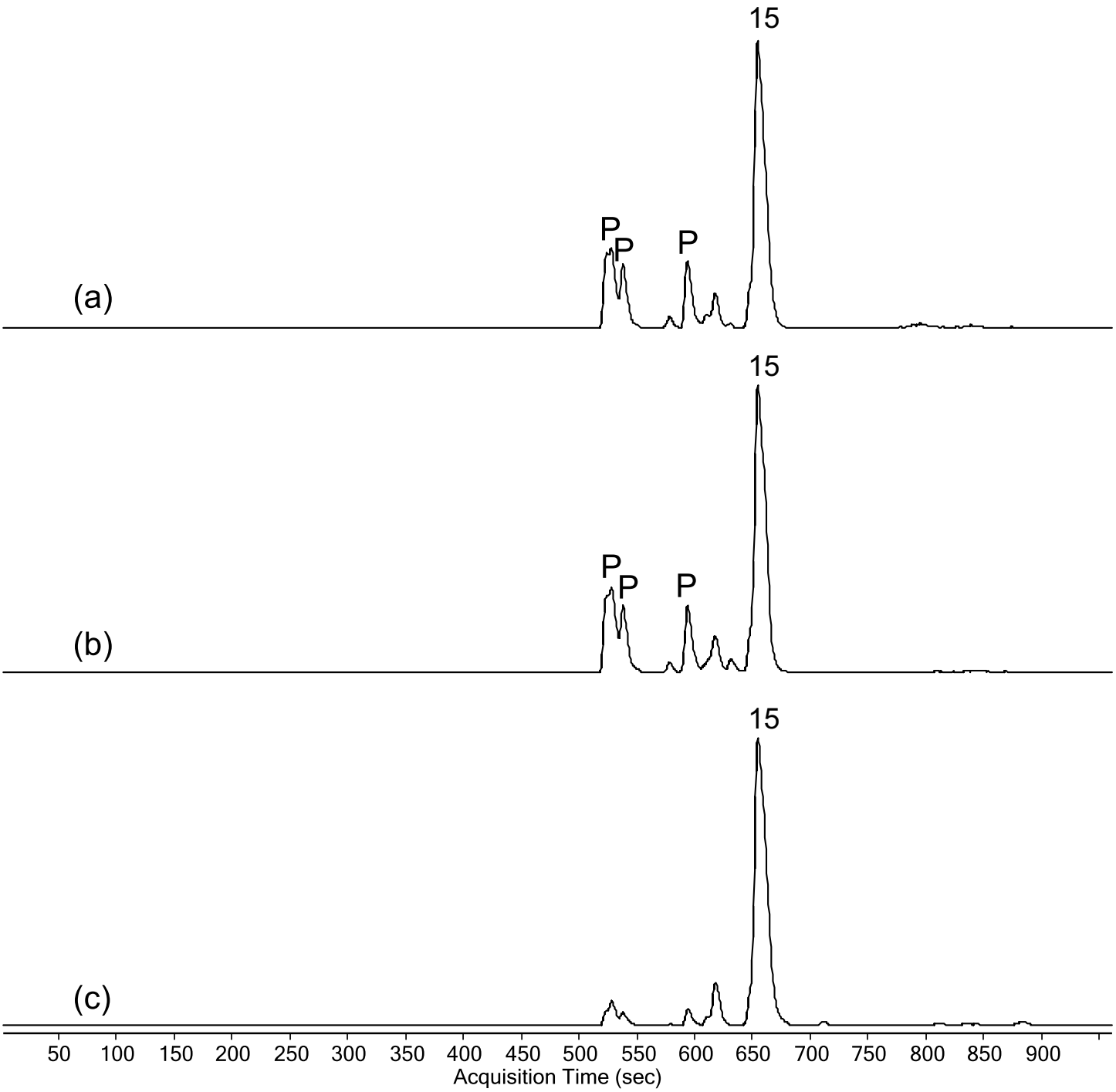

Figure S19. Q-TOF LC-MS analysis depicting EICs of (a) NotI′ reaction with notoamide S (**15**); (b) NotI reaction with **15**; (c) no enzyme control with **15**. Product(s) formed are denoted with **P**. Data were measured on an Agilent Q-TOF LC-MS.

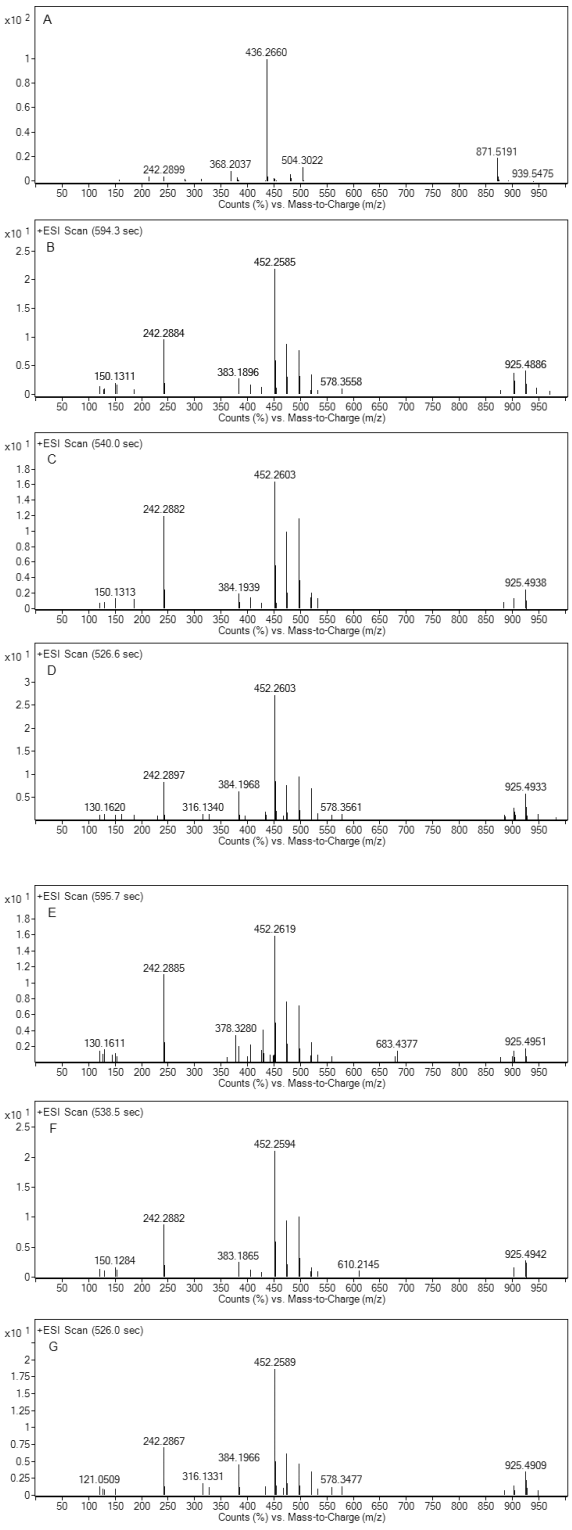

Figure S20. Mass spectra of (A) notoamide S (**15**) standard, expected $[M+H]^+$ = 436.2600; (B) Product formed from reaction of NotI with **15** observed at 594.3 seconds; (C) Product formed from reaction of NotI with **15** observed at 540.0 seconds; (D) Product formed from reaction of NotI with **15** observed at 526.6 seconds; (E) Product formed from reaction of NotI′ with **15** observed at 595.7 seconds; (F) Product formed from NotI′ in reaction with **15** observed at 538.5 seconds; (G) Product formed from NotI′ in reaction with **15** observed at 526.0 seconds. Oxidized products have an expected $[M+H]^+$ of 452.2549. Data were measured on an Agilent Q-TOF LC-MS.

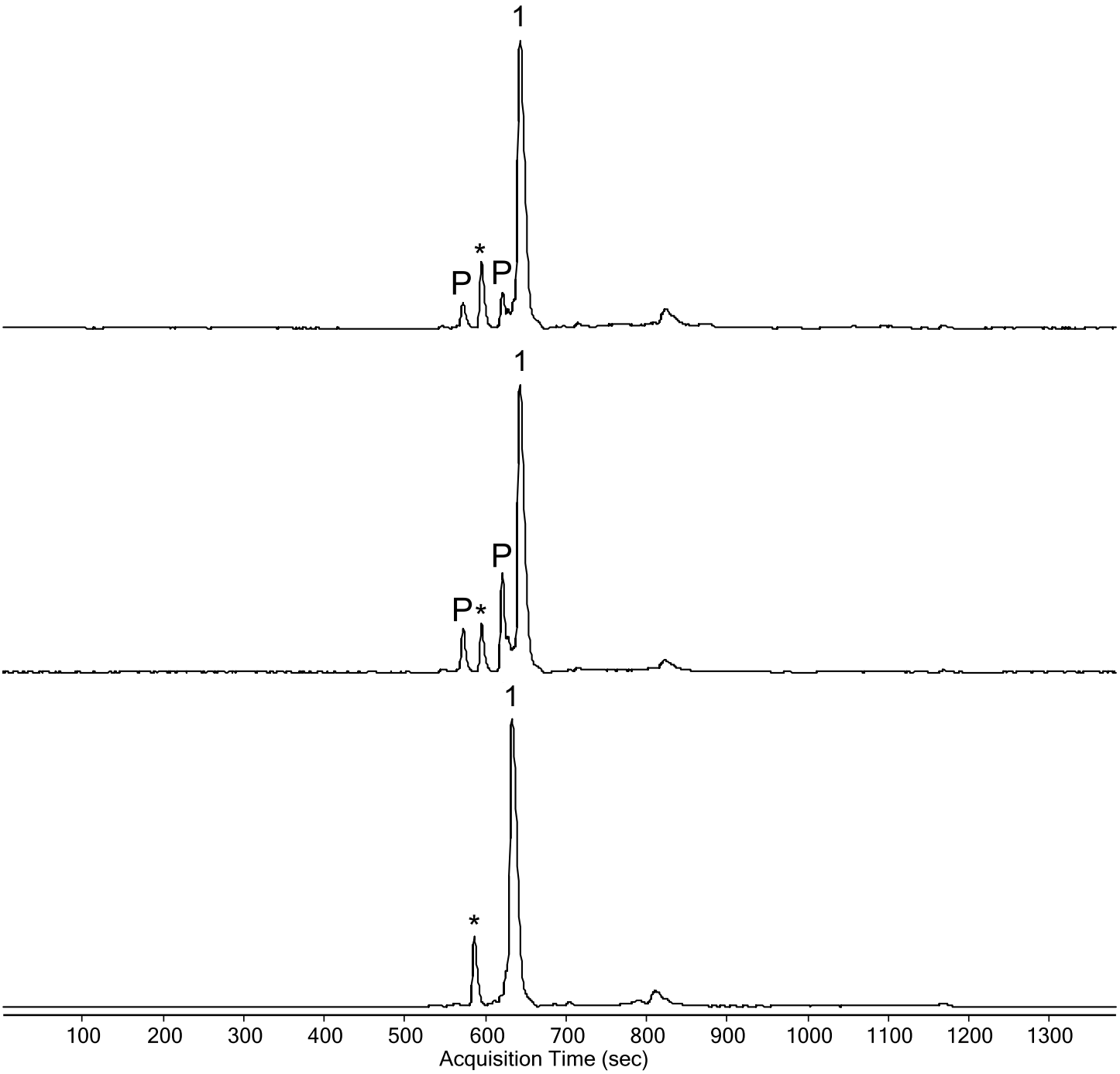

Figure S21. Q-TOF LC-MS analysis depicting EICs of (a) NotI′ reaction with notoamide E (**1**); (b) NotI reaction with **1**; (c) no enzyme control with **1**. Products formed are denoted with **P**. Asterisk denotes possible diastereomer of **1**. Data were measured on an Agilent Q-TOF LC-MS.

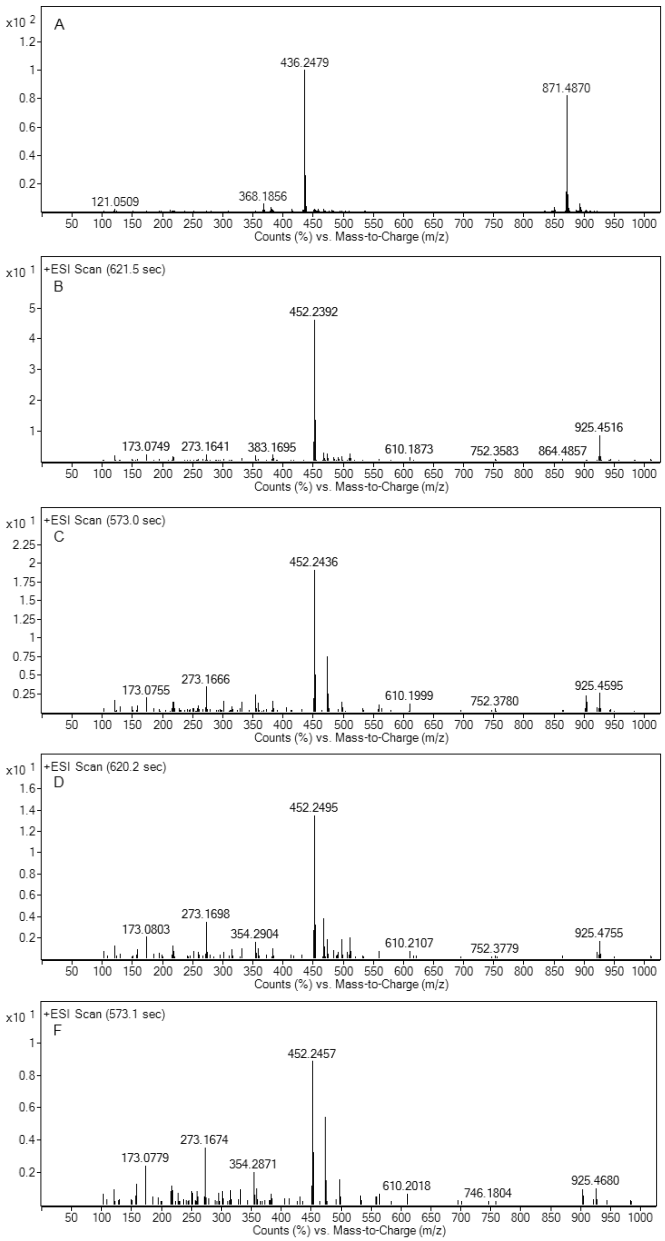

Figure S22. Mass spectra of (A) notoamide E (**1**) standard labelled with two ^{13}C atoms, expected $[M+H]^+$ = 436.2444; (B) Product formed from reaction of NotI with **1** observed at 621.5 seconds; (C) Product formed from reaction of NotI with **1** observed at 573.0 seconds; (D) Product formed from reaction of NotI′ with **1** observed at 620.2 seconds; (E) Product formed from reaction of NotI′ with **1** observed at 573.1 seconds. Oxidized products have an expected $[M+H]^+$ of 452.2393. Data were measured on an Agilent Q-TOF LC-MS.

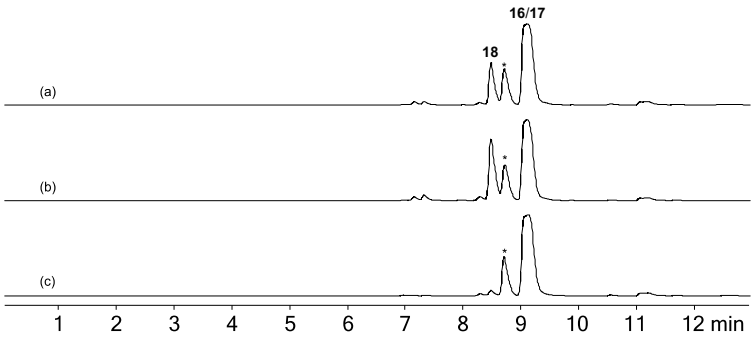

Figure S23. Q-TOF LC-MS analysis depicting EICs of (a) NotI reaction with notoamide T (**16**/**17**); (b) NotI′ reaction with **16**/**17**; (c) No enzyme control with **16**/**17**. Products formed are denoted with **18** (notoamide TI). Asterisk denotes possible diastereomers of **16**/**17**. Data were measured on an Agilent Q-TOF LC-MS.

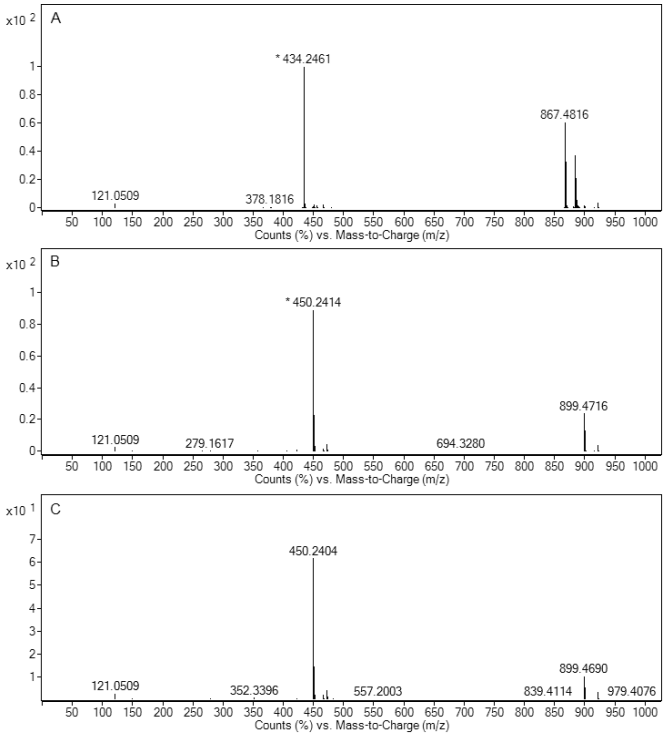

Figure S24. Mass spectra of (A) (+)- and (-)-notoamide T (**16** and **17**) standards in racemic mixture, expected $[M+H]^+$ = 434.2444; (B) Product formed from reaction of NotI with the racemic **16**/**17**, expected $[M+H]^+$ = 450.2392; (C) Product formed from reaction of NotI′ with the racemic **16**/**17**, expected $[M+H]^+$ = 450.2392. Data were measured on an Agilent Q-TOF LC-MS.

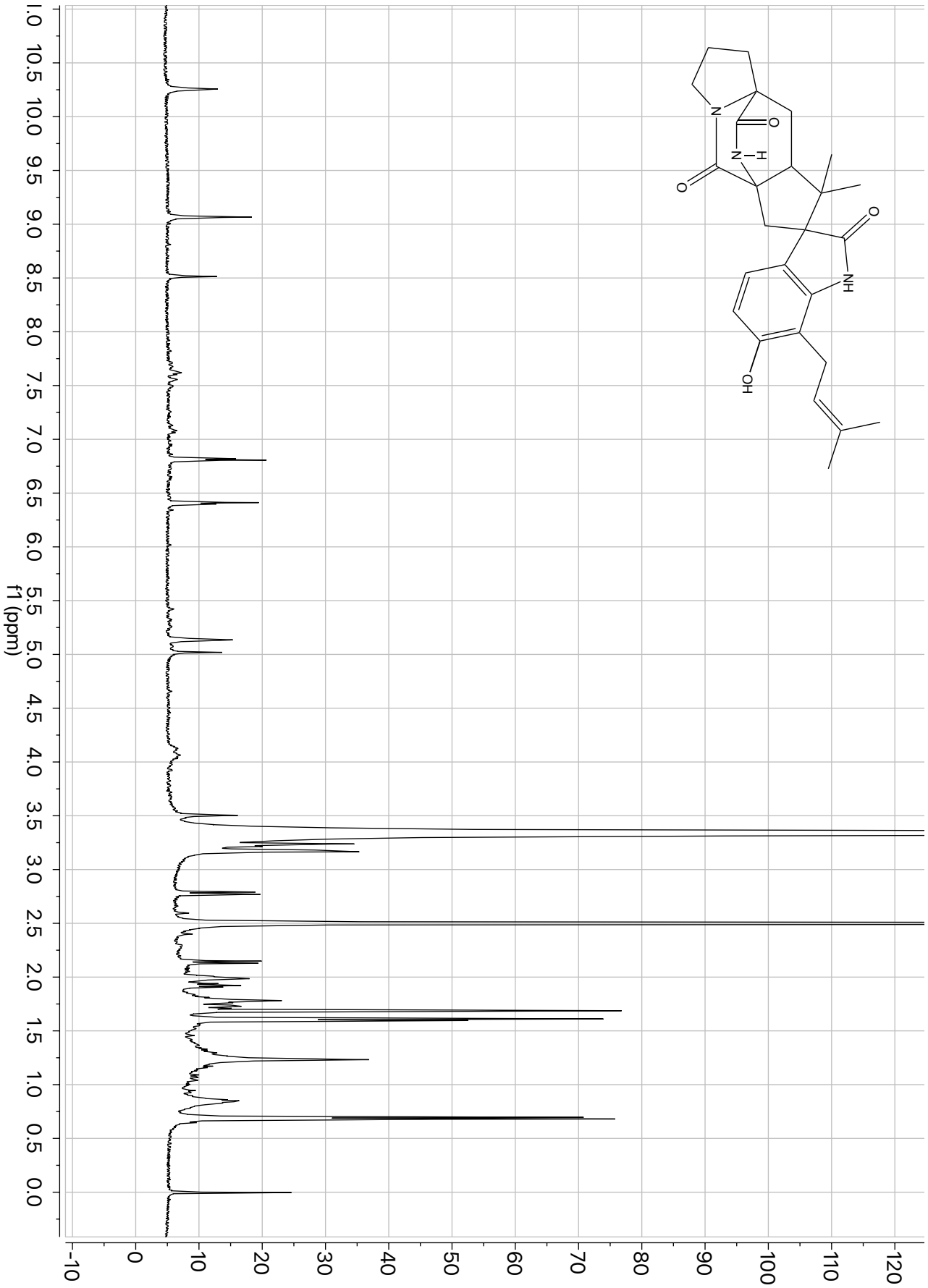

Figure S25. ^{1}H-NMR spectrum of Notoamide TI (**18**) recorded at 700 MHz in $(CD_3)_2SO$-d_6.

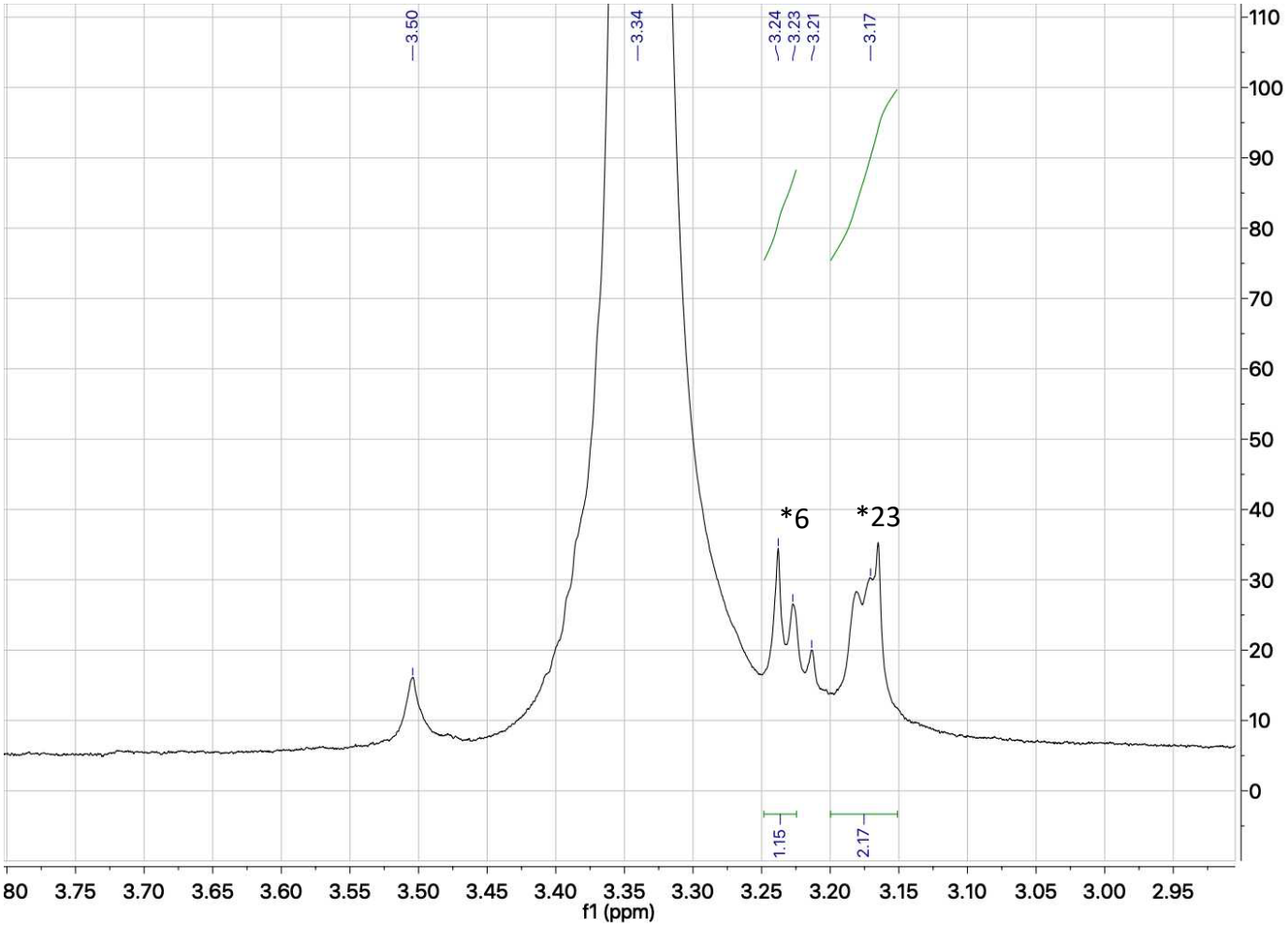

Figure S26. Zoomed view of ^{1}H-NMR spectrum of Notoamide TI (**18**) recorded at 700 MHz in $(CD_3)_2SO$-d_6 to show multiplets at 3.17ppm (CH_2, position 23) and 3.24ppm (CH, position 6).

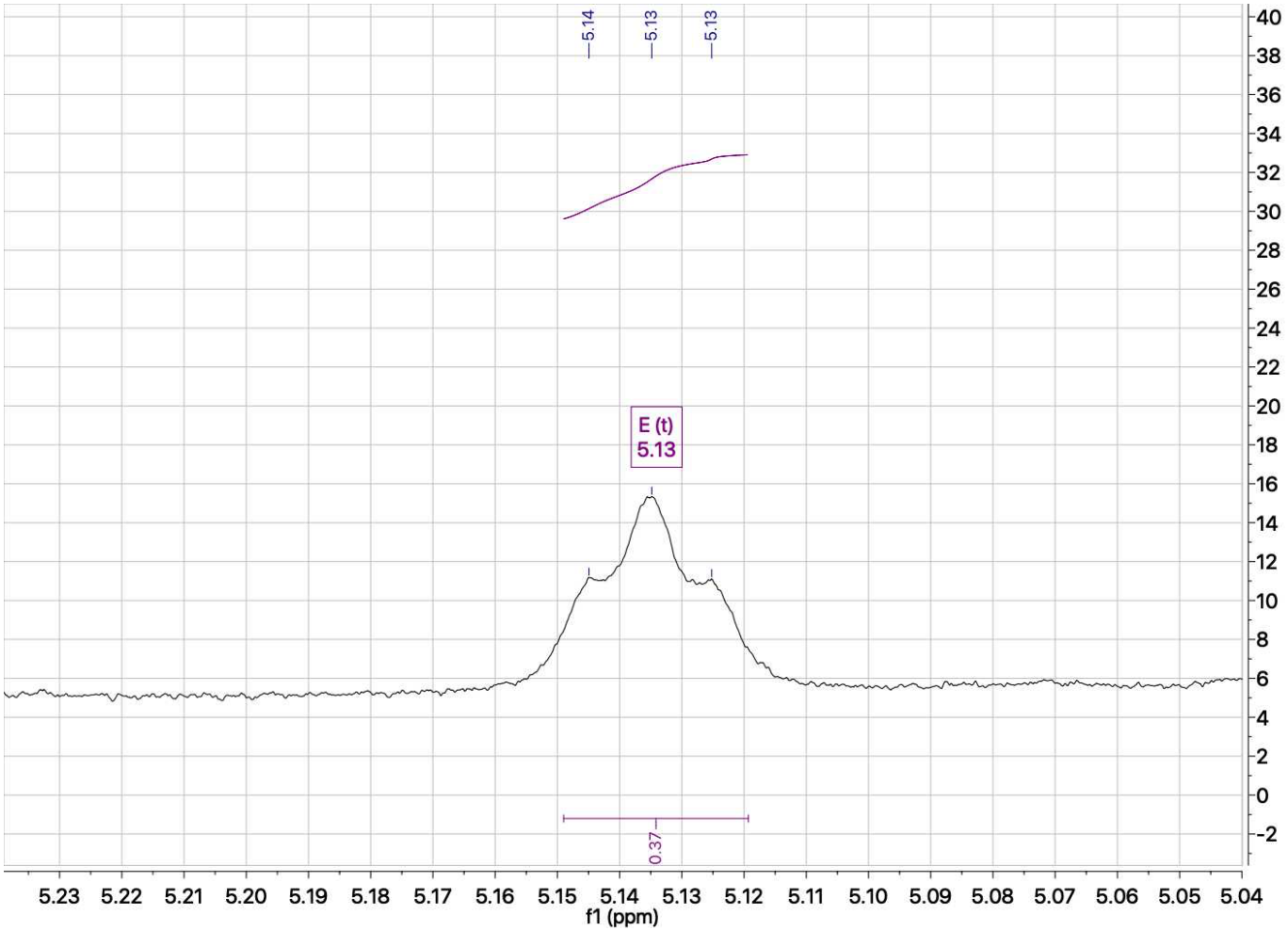

Figure S27. Zoomed view of ^{1}H-NMR spectrum of Notoamide TI (**18**) recorded at 700 MHz in $(CD_3)_2SO$-d_6 to show a triplet at 5.13 ppm (CH, position 24).

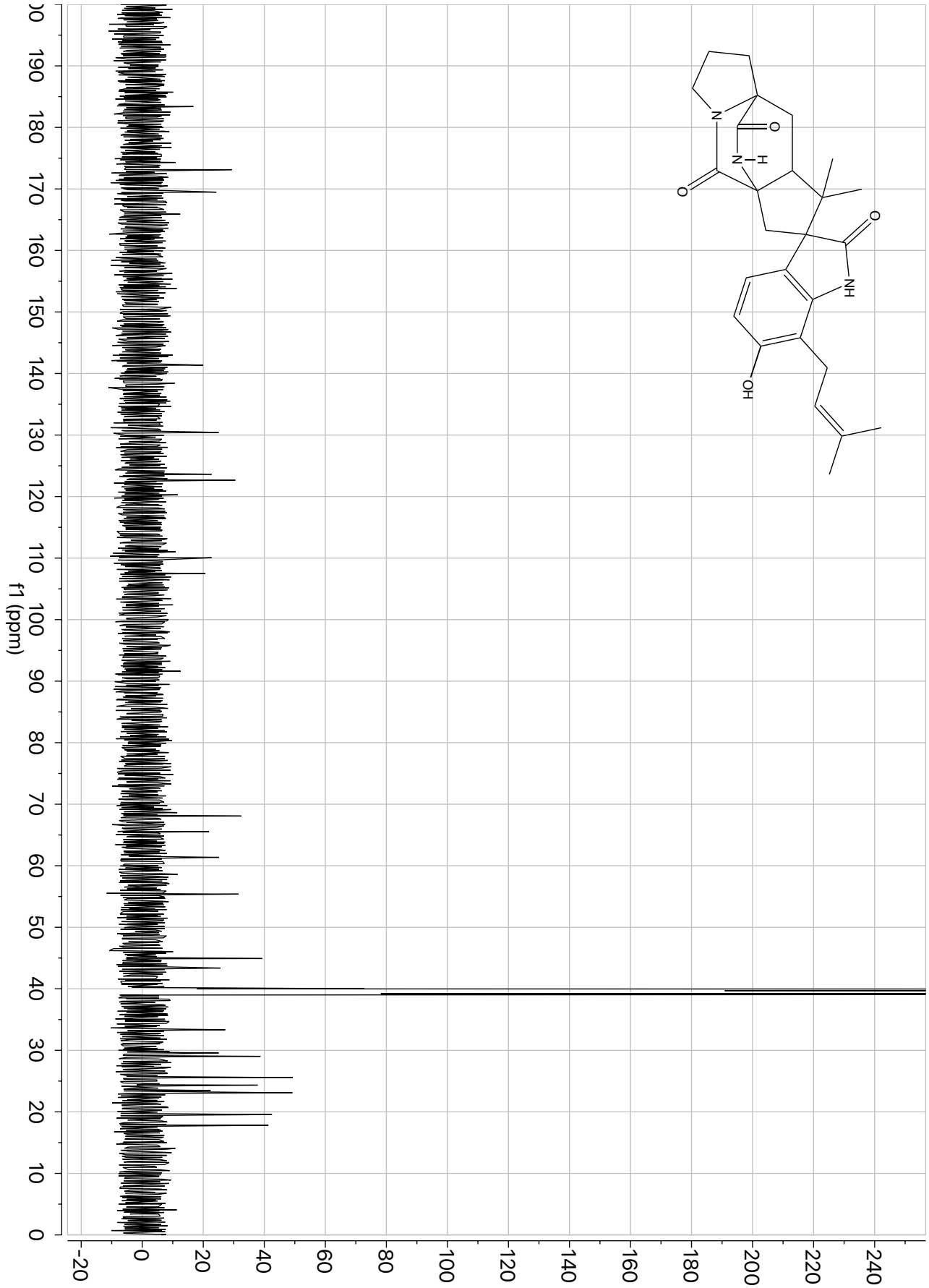

Figure S28. ^{13}C-NMR spectrum of Notoamide TI (**18**) recorded at 176 MHz in $(CD_3)_2SO$-d_6.

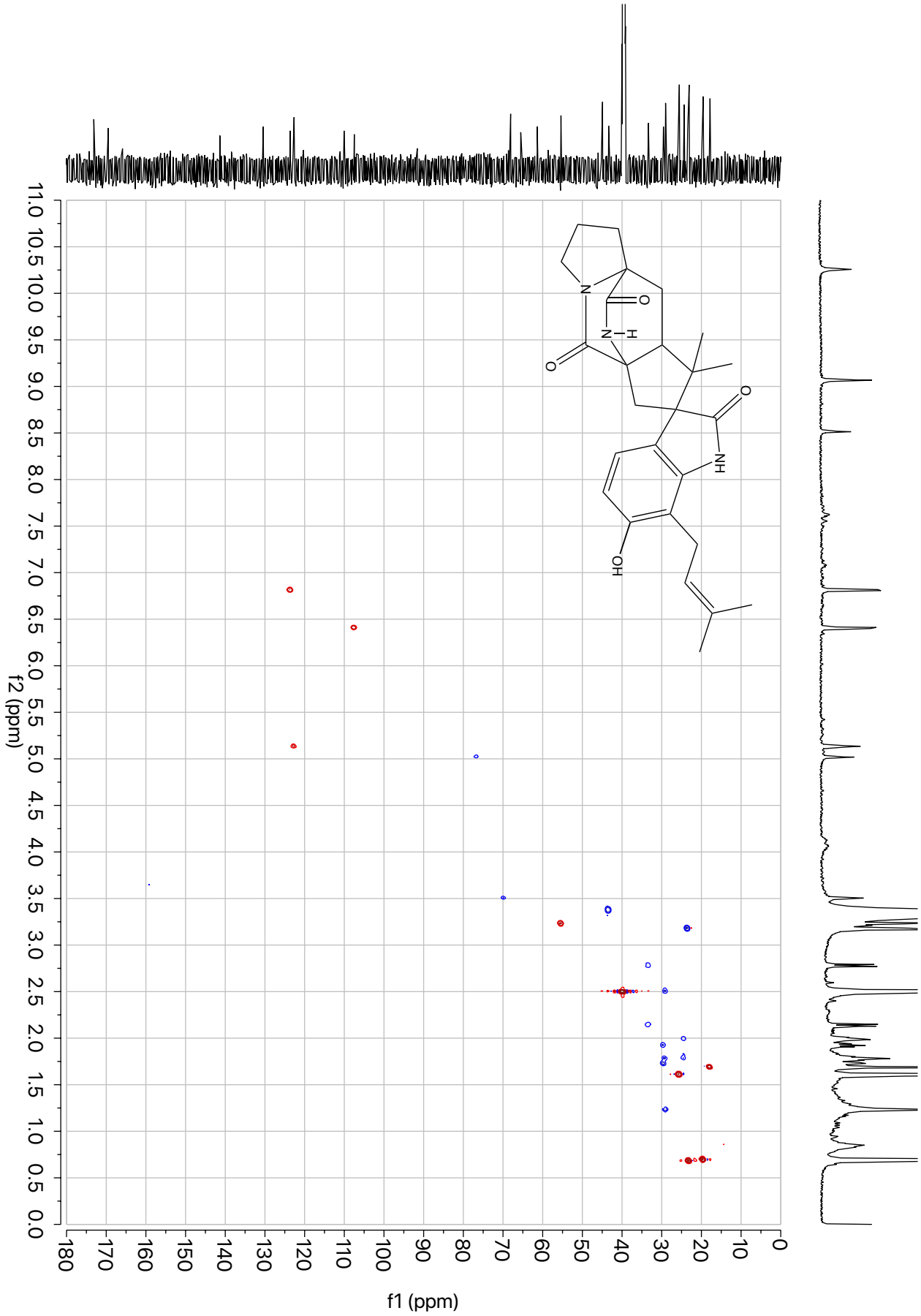

Figure S29. gHSQCAD spectrum of Notoamide TI (**18**) recorded at 700 MHz in $(CD_3)_2SO$-d_6.

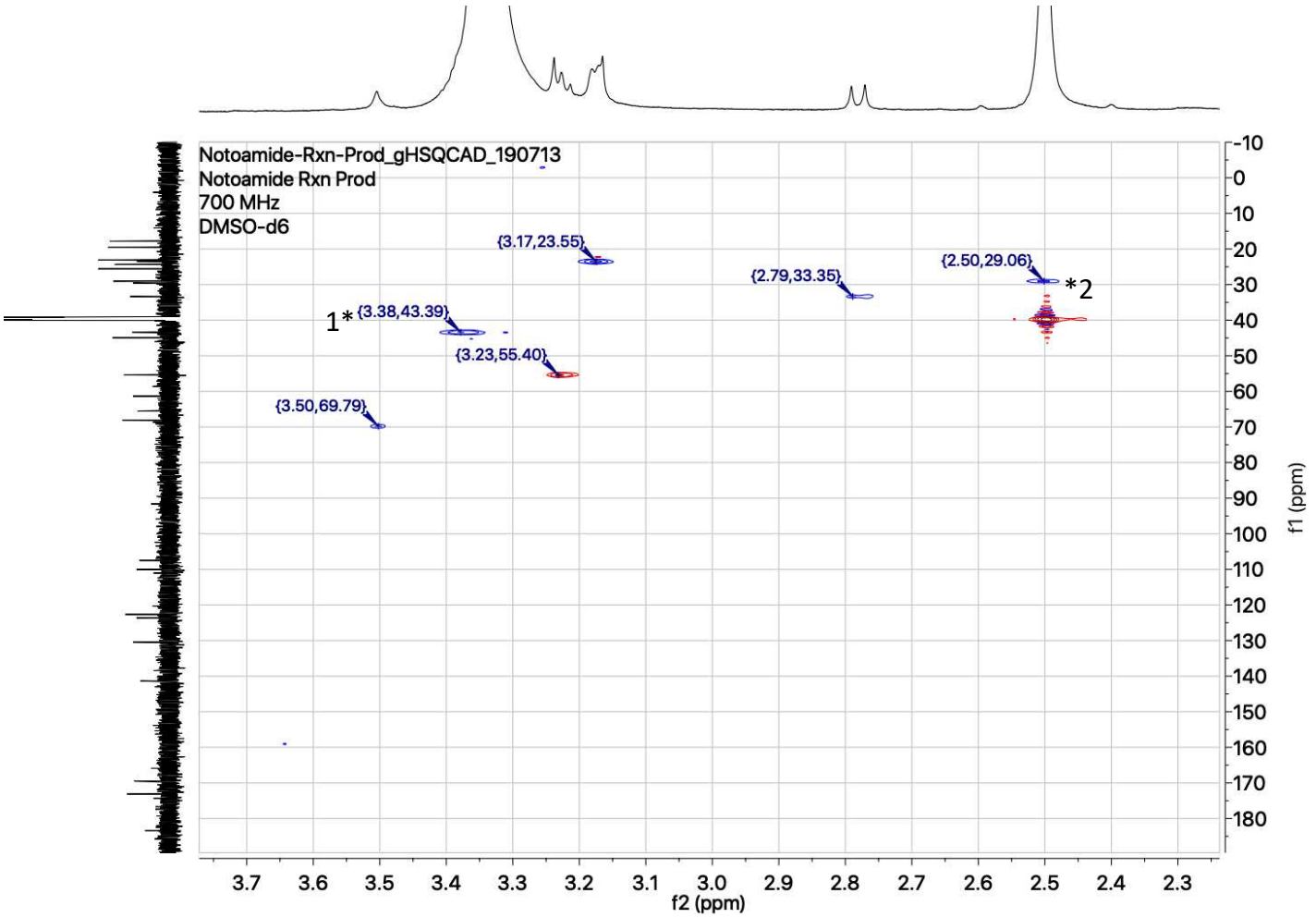

Figure S30. Zoomed view of the gHSQCAD spectrum of Notoamide TI (**18**) recorded at 700 MHz in $(CD_3)_2SO$-d_6 to display the solvent-obscured peaks at (C2, 2.50/29.06 ppm) and (C1, 3.38/43.39 ppm). The peaks for positions 2 and 1 are indicated with asterisks.

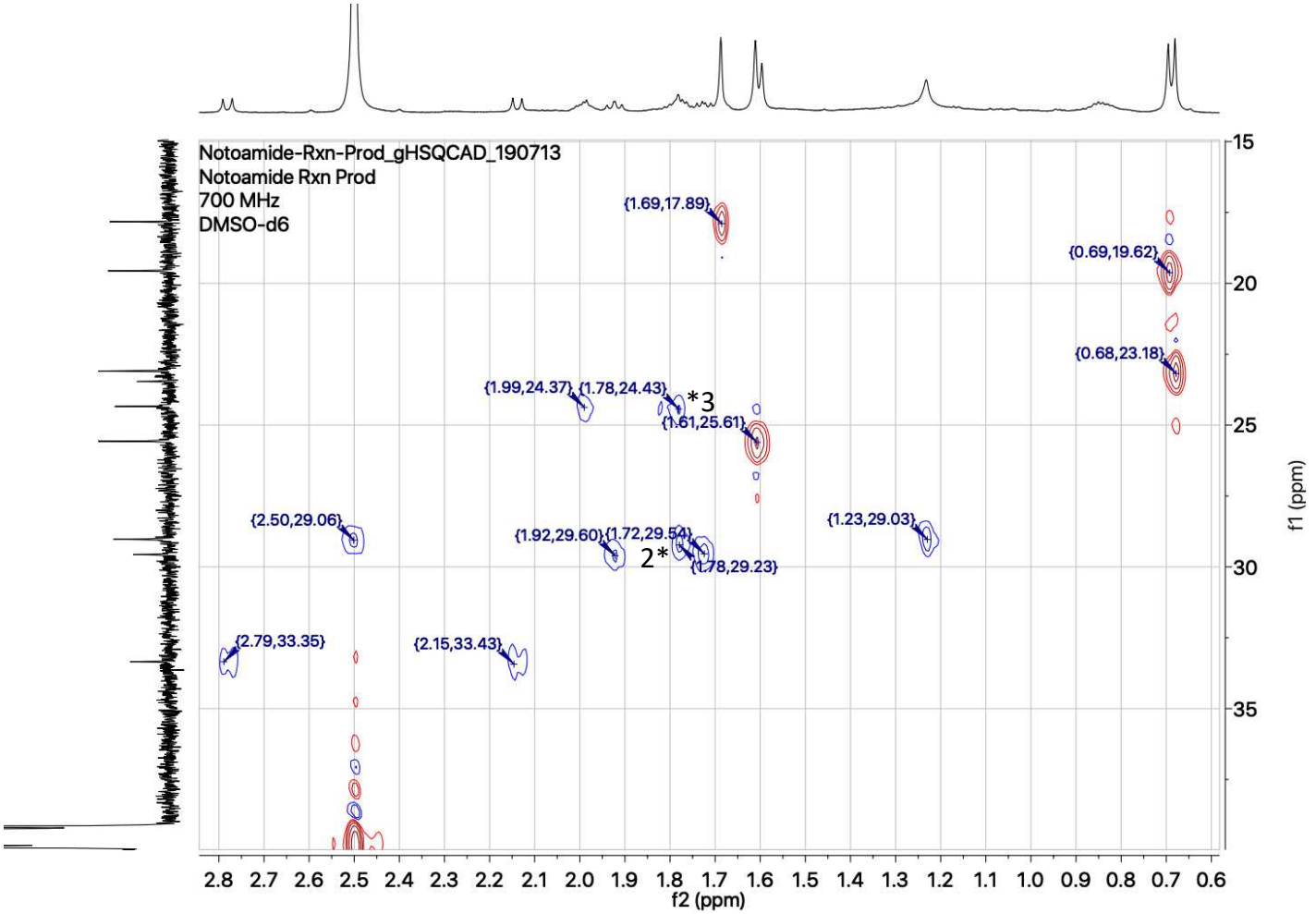

Figure S31. Zoomed view of the gHSQCAD spectrum of Notoamide TI (**18**) recorded at 700 MHz in $(CD_3)_2SO$-d_6 to display the peaks for C2 and C3, for which the proton signals overlap at 1.78. The peaks for positions 2 and 3 are indicated with asterisks.

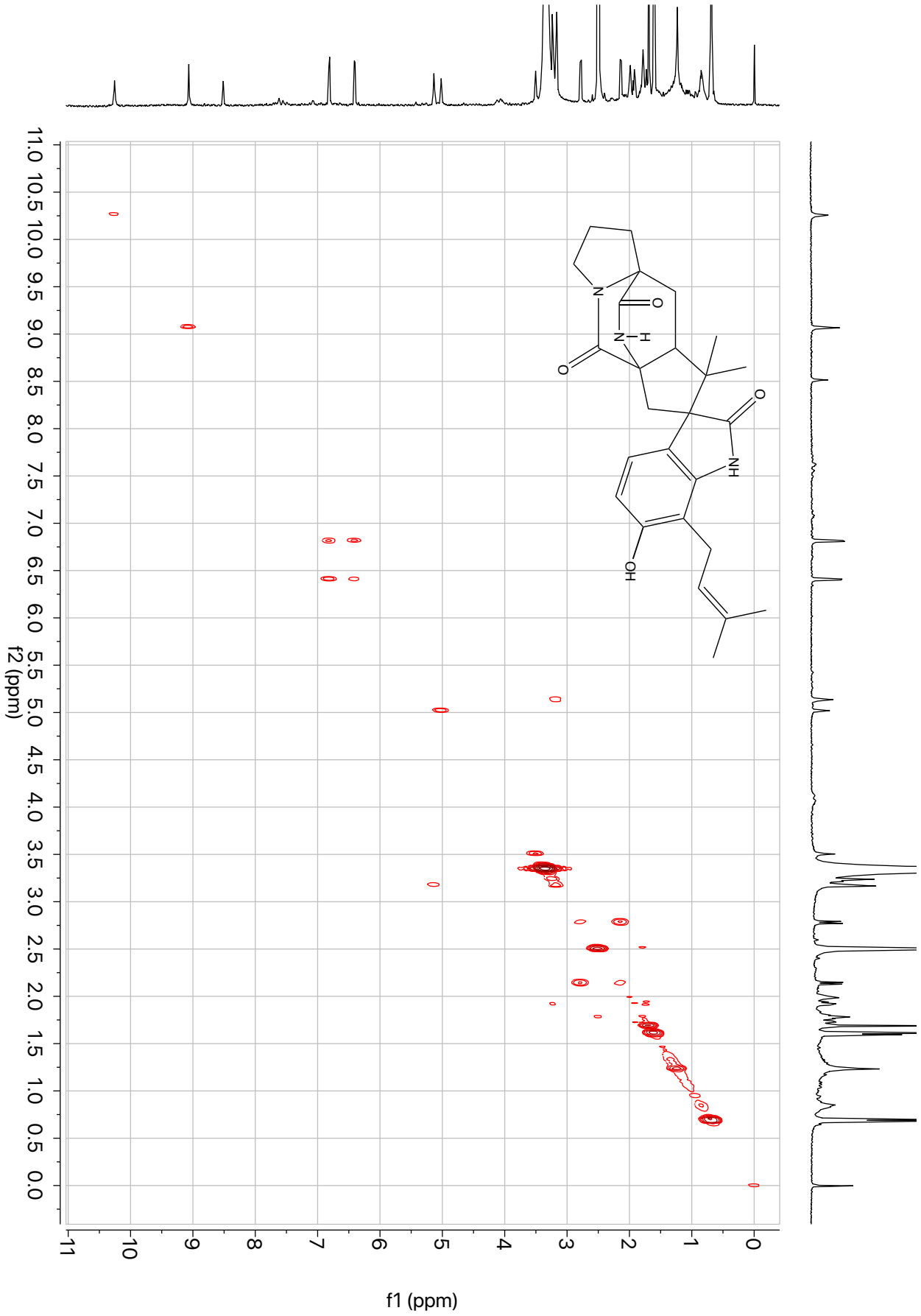

Figure S32. gCOSY spectrum of Notoamide TI (**18**) recorded at 700 MHz in $(CD_3)_2SO$-d_6.

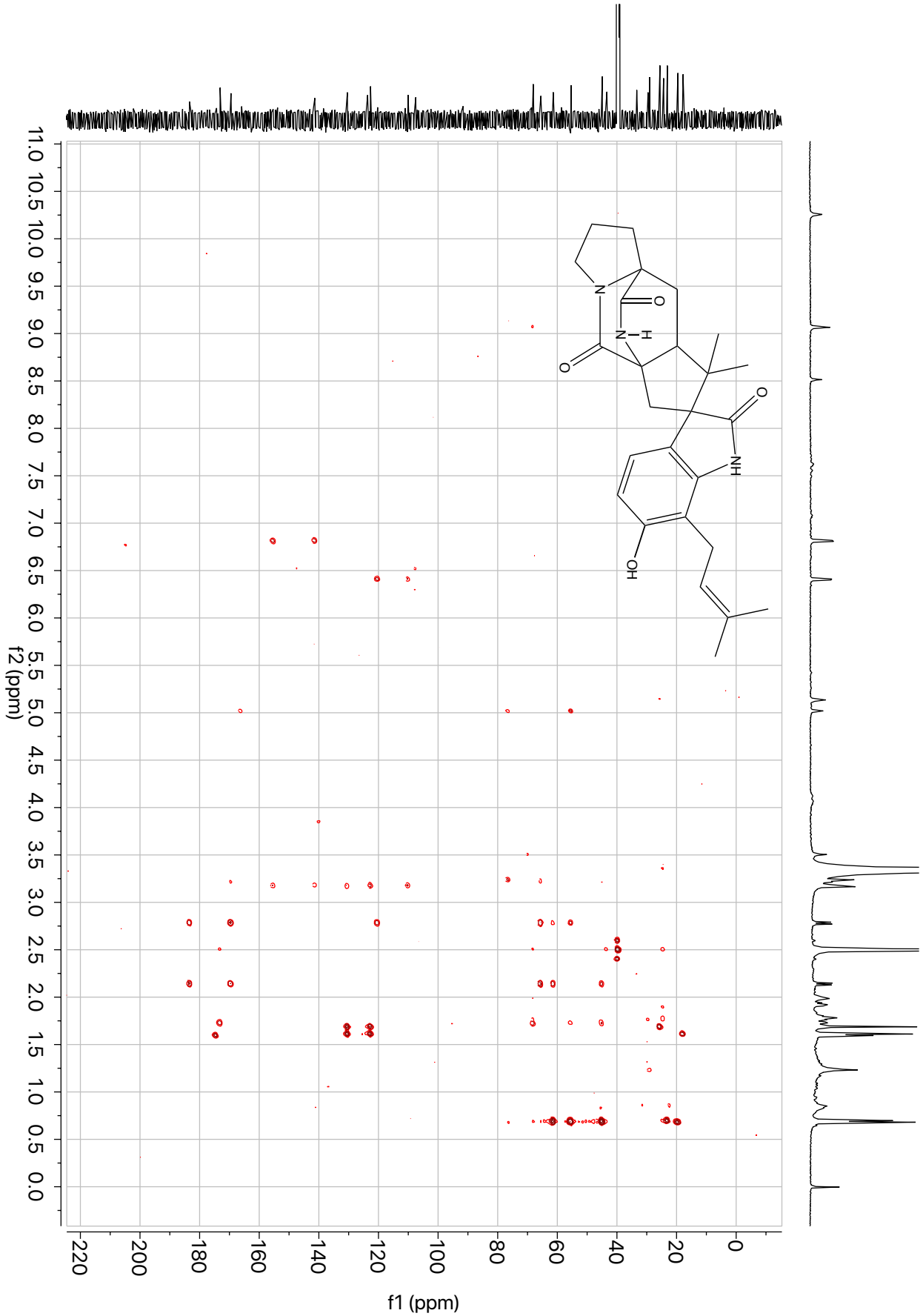

Figure S33. gHMBCAD spectrum of Notoamide TI (**18**) recorded at 700 MHz in $(CD_3)_2SO$-d_6.

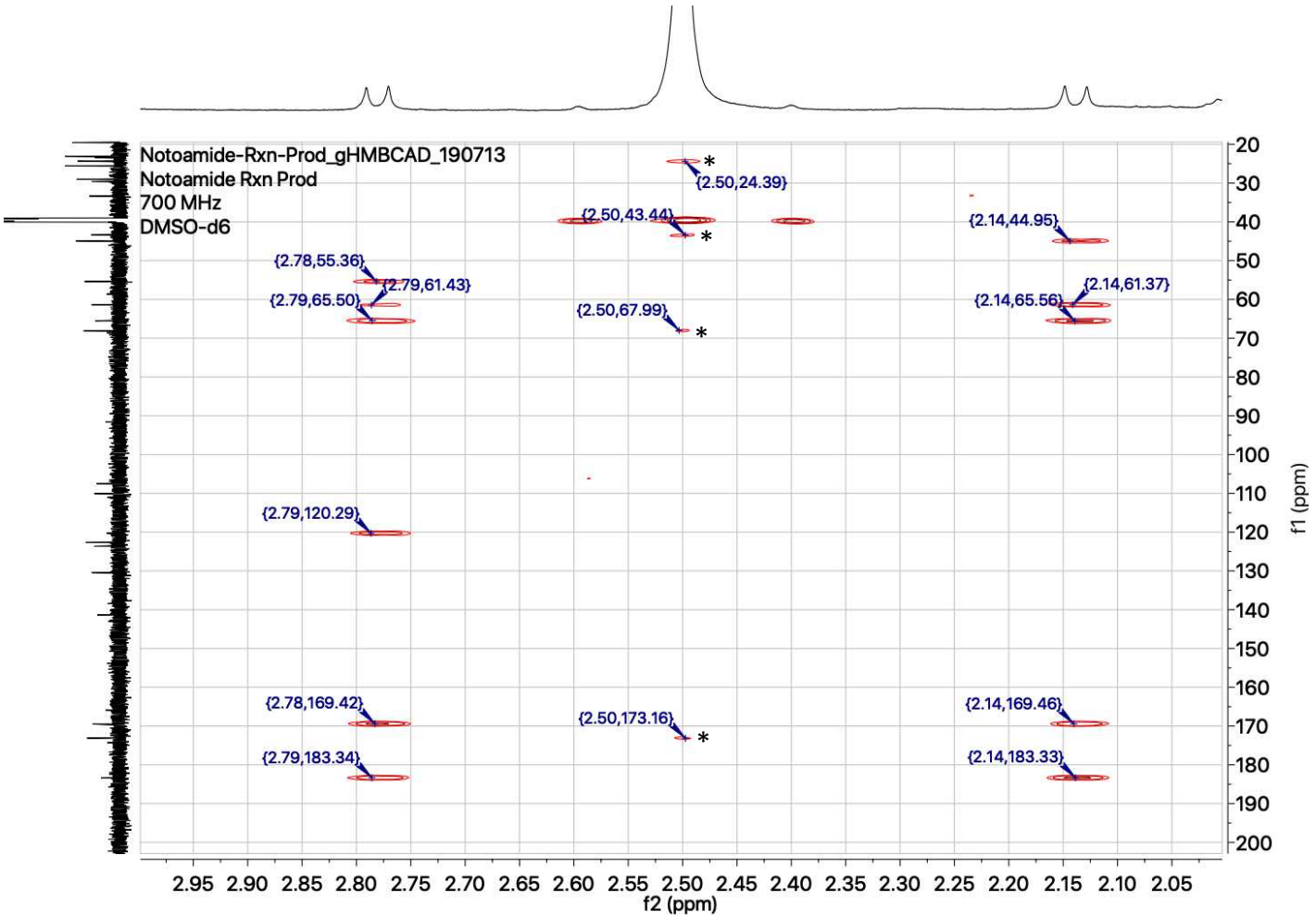

Figure S34. Zoomed view of the gHMBCAD spectrum of Notoamide TI (**18**) recorded at 700 MHz in $(CD_3)_2SO$-d_6 to display the correlations from the solvent-obscured peak at 2.50 ppm (indicated by asterisks).

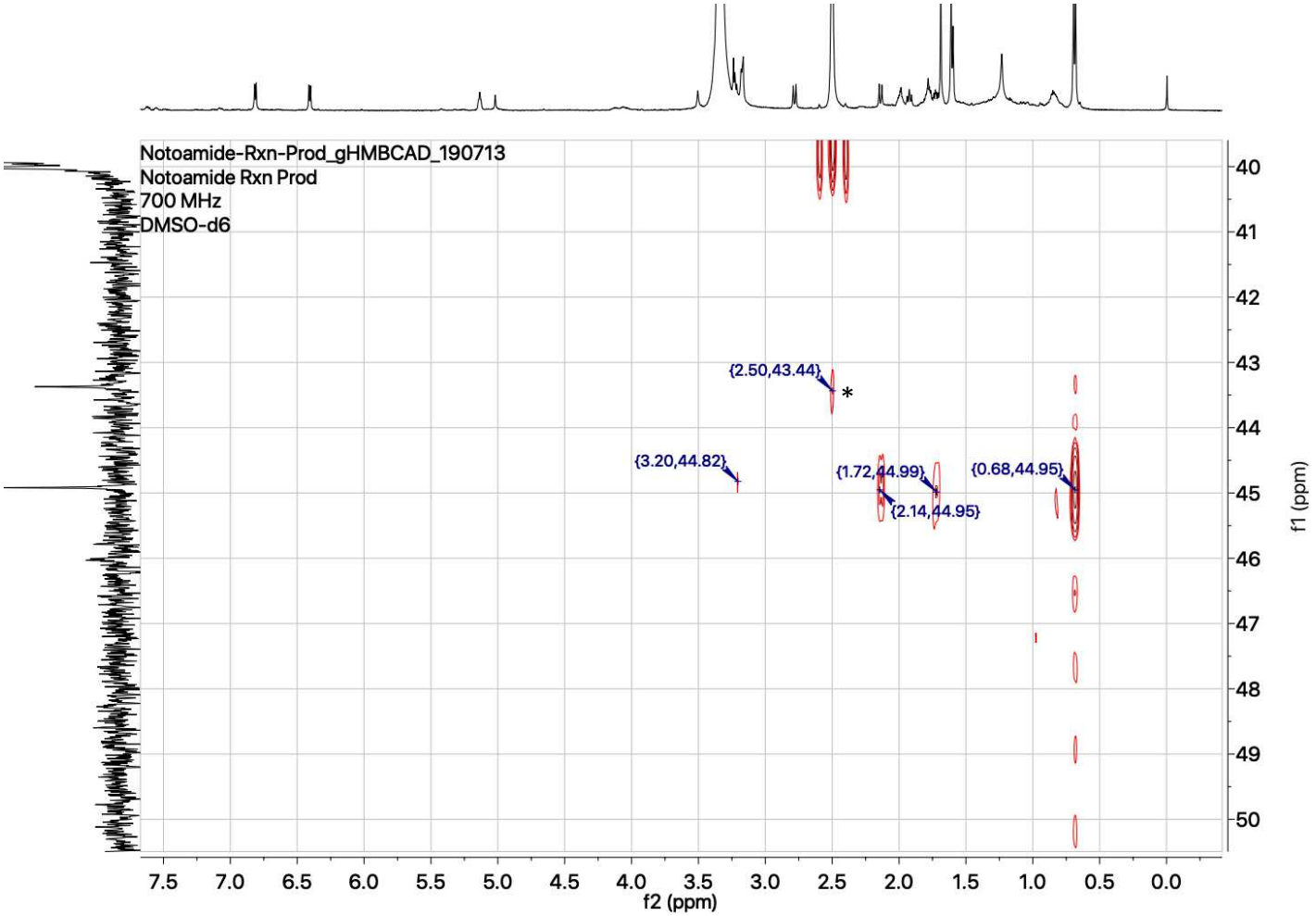

Figure S35. Zoomed view of the gHMBCAD spectrum of Notoamide TI (**18**) recorded at 700 MHz in $(CD_3)_2SO$-d_6 to display the correlations from the solvent-obscured peak at 2.50 ppm to C2, indicated by an asterisk.

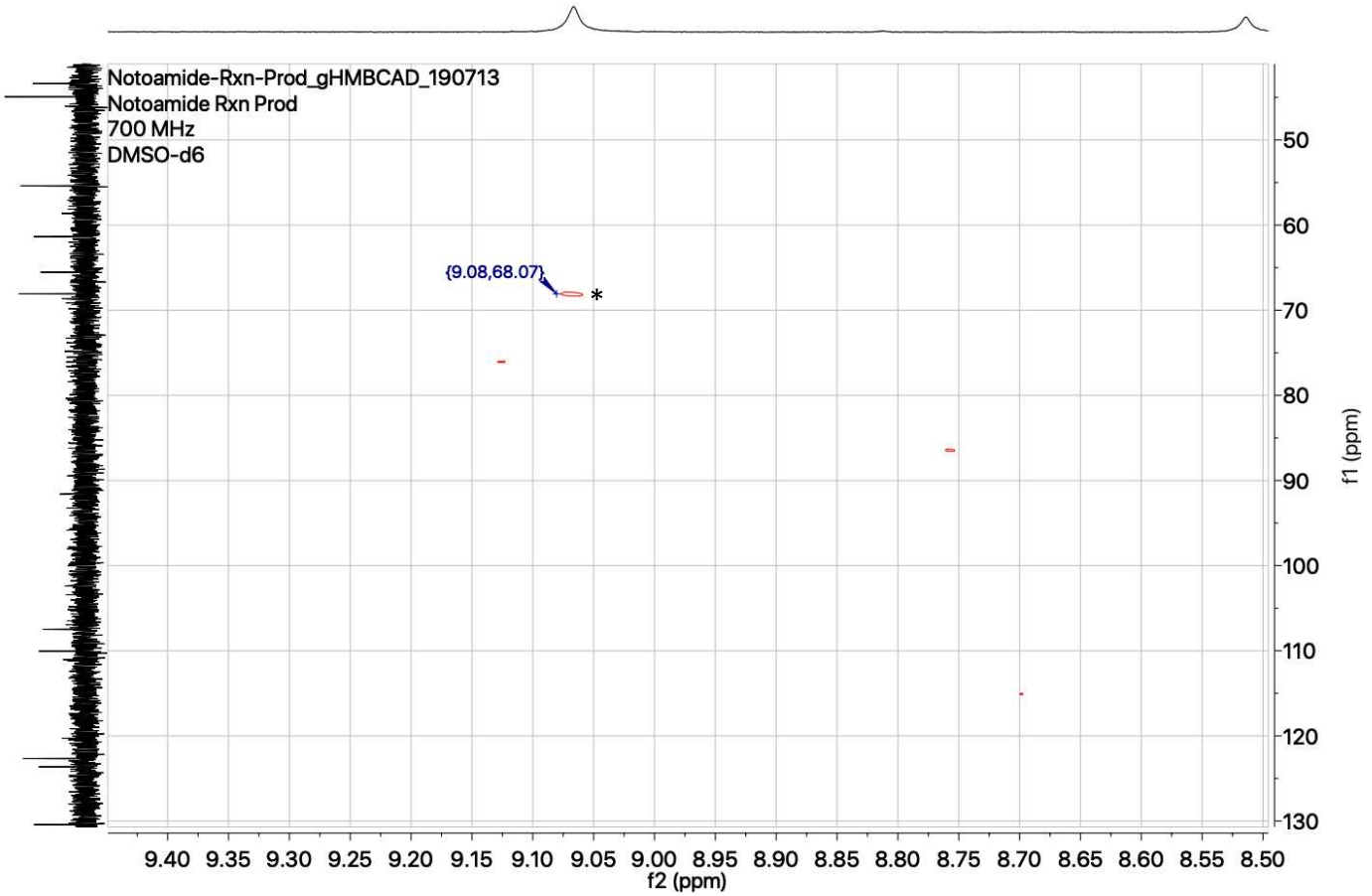

Figure S36. Zoomed view of the gHMBCAD spectrum of Notoamide TI (**18**) recorded at 700 MHz in $(CD_3)_2SO$-d_6 to display the correlations from NH(22) at 9.07ppm to C4 at 68.07ppm, indicated by an asterisk.

References

[1] D. Pistorius, Y. Y. Li, A. Sandmanny, R. Muller, *Mol Biosyst* **2011**, *7*, 3308-3315.

[2] A. E. Fraley, K. Caddell Haatveit, Y. Ye, S. P. Kelly, S. A. Newmister, F. Yu, R. M. Williams, J. L. Smith, K. N. Houk, D. H. Sherman, *J. Am. Chem. Soc.* **2020**, *142*, 2244-2252.

[3] S. A. Newmister, C. M. Gober, S. Romminger, F. Yu, A. Tripathi, L. L. L. Parra, R. M. Williams, R. G. S. Berlinck, M. M. Joullié, D. H. Sherman, *J. Am. Chem. Soc* **2016**, *138*, 11176-11184.

[4] S. Y. Li, J. M. Finefield, J. D. Sunderhaus, T. J. McAfoos, R. M. Williams, D. H. Sherman, *J Am Chem Soc* **2012**, *134*, 788-791.

[5] Y. Ye, L. Du, X. Zhang, S. A. Newmister, W. Zhang, S. Mu, A. Minami, M. McCauley, J. V. Alegre-Requena, A. E. Fraley, M. L. Androver-Castellano, V. V. Shende, H. Oikawa, H. Kato, S. Tsukamoto, R. Paton, R. M. Williams, D. H. Sherman, S. Li, *ChemRxiv* **2019**.

[6] F. Madeira, Y. M. Park, J. Lee, N. Buso, N. Madhusoodanan, P. Basutkar, A. R. N. Tivey, S. C. Potter, R. D. Finn, R. Lopez, *Nucleic Acids Research* **2019**, *47*, W636-W641.

[7] M. H. M. Eppink, H. A. Schreuder, W. J. H. van Berkel, *Protein Sci* **1997**, *6*, 2454-2458.